Special Purpose Attachment for Rotorcraft Cooperative Lift (SPARCL)

Submission to the 2010 AHS Student Design Competition

6/1/2010

The Pennsylvania State University

Greg Beres
Alex Carrasquillo
Austin Cornell
Lahiru Fernando
James Krouse
Jake Marsh
Edwin Reynolds
Emily Wallis

Table of Contents

Acknowledgements

The SPARCL design team would like to thank the following individuals for their invaluable help during the design process:

Dr. Robert Bill
Dr. Joe Horn
Dr. Edward Smith
Dr. Chris Rahn
Jose Palacios
Sreeni Narayanan

Signatures

Greg Beres

Edwin Reynolds

Alex Carrasquillo

Emily Wallis

Austin Cornell

Dr. Robert Bill – Faculty Advisor

Lahiru Fernando

Dr. Joseph Horn – Faculty Advisor

James Krouse

Dr. Edward Smith – Faculty Advisor

Jake Marsh

All students received five hours of academic credit for participating in the 2010 AHS Student Design Competition. These credits were divided between two classes: AERSP 402A Helicopter Design – Preliminary (3) and AERSP 402B Helicopter Design – Detailed (2)

1 RFP Compliance

Base aircraft 5,000 lb useful load capability	19,200 lbs useful load
Current in-service aircraft	1,200+ CH-47 in service
100nm delivery distance capable	Capable (Performance section)
Mid-point hover for 10 minutes	Capable (Performance section)
Return without payload	Capable (Performance section)
Load handling structure	Spreader Bar, Load capable (Structures Section)
Multi-aircraft stability	LQR feedback system (Dynamics Section)
Takeoff and landing techniques	Mission capable (Operational Procedure)
Aircraft control coordination	Coordinated waypoints (Operational Procedure)
Ability to lift 75% more payload weight than either helicopter alone	Capable (Performance section)

2 Introduction

The idea of using more than one helicopter to lift a heavy load is not a recent development. One method is to rigidly attach the two helicopters together, creating essentially a single helicopter. In 1972, Piasecki Aircraft Corporation conducted a feasibility study on rigidly attaching two CH-53D helicopters in various arrangements. The two helicopters were heavily modified with a tubular structure connecting the two rotorcraft. A transmission shaft between the two helicopters ensured safety with power transfer during emergency conditions. The most feasible configuration was nose to tail arrangement, that is, the nose of the rear helicopter is attached to the tail of the forward helicopter. This design required the removal of the empennage and tail rotor of the forward helicopter and heavy modification to the transmission and flight control system of both helicopters to allow shared transmission and flight controls.

Another Piasecki Patent in 1972 also briefly described a multiple helicopter lift system using two or three CH-47 Chinooks. Similar to the earlier feasibility study, the CH-47s were rigidly attached to each other, with each aircraft's transmission and control systems linked together in a similar manner.

A more unique design in the 1980's was Piasecki's PA-97 Helistat prototype. The design used the conjunction of a blimp and four helicopters for greatly increased lifting capabilities. The 1986 demonstrator aircraft used a Navy ZPG-2W blimp and four H-34J helicopters. The helicopters were substantially modified and attached to a tubular structure incorporating the blimp. However, the demonstrator aircraft crashed on July 1st, 1986 due to mechanical vibrations caused by the undercarriage and helicopter vibrations.

Flight test demonstrations of the twin-lift concept were conducted in the late 1970s and early 1980s by PLM Helicopters in Scotland using Bell Jet Rangers, Peninsula Helicopters using the Hiller 5000 helicopters, Sikorsky Aircraft with two CH-54s and by the Soviets using the MIL-26 helicopters. While early demonstrations proved twin lift was possible, a large pilot workload made feasible operation limited.

3 RFP Requirements

> "A technology demonstrator multi-lift system is to be designed such that two rotorcraft can be cooperatively operated to lift 75% more payload than either aircraft alone could lift. Enough fuel needs to be aboard at takeoff for a 100nm delivery distance, mid-point hover capability for 10minutes, and return without the payload.
> The focus is to be on the system concept – load lifting devices, control scheme, and multi-aircraft system stability – rather than a particular aircraft or payload. Therefore, a current, in-service rotorcraft should be selected as the baseline aircraft to design the concept and technologies involved. The baseline aircraft should have at least 5,000 lb useful load capability at Sea Level/ISA +20° conditions.
> Design and Analysis must address the load handling device/structure, load sharing between the aircraft, multi-aircraft stability, Take-Off and Landing Techniques, and Aircraft control coordination. Any mechanical or electronic modifications necessary for the baseline aircraft, system redundancy, and other safety considerations should also be addressed.
> A production Heavy Multi-Lift load handling system would be able to accommodate 20' and 48' ISO containers, various wheeled or tracked vehicles, and large construction machinery. Dependent on the baseline aircraft chosen, a proportionally sized load handling device should be defined for perspective payloads.

4 Configuration Selection

4.1 Rigid

Rigid configuration refers to having the two helicopters rigidly connected to each other by the way of structural modification. This may include heavy modification of one or more helicopters and complex transmission linkages. To structurally connect two aircraft together, the aircraft must be stripped to provide suitable attachments points, entire sections of the aircraft may have to be removed, such as the rear empennage of the forward helicopter in a longitudinal fore-to-aft configuration. Due to the nature of such a configuration, the event of an engine malfunction must be addressed as well.

A transmission linkage between to two helicopters must be used to adequately transfer power and respond to situations such as loss of an engine. This requires modification to the existing helicopter transmission system and a driveshaft or transmission system in the connecting structure itself to transfer power from one aircraft to the other.

The third major modification is to the flight control system. As the two helicopters are rigidly attached, neither will behave in a manner similar to the helicopter pre-modification, rather the two helicopters will behave as a single helicopter with new flight characteristics possibly resembling a tandem-rotor helicopter like the CH-47 Chinook. Because of the extensive airframe and propulsion modifications required, a rigid connection system was deemed to be too complicated for use on this project.

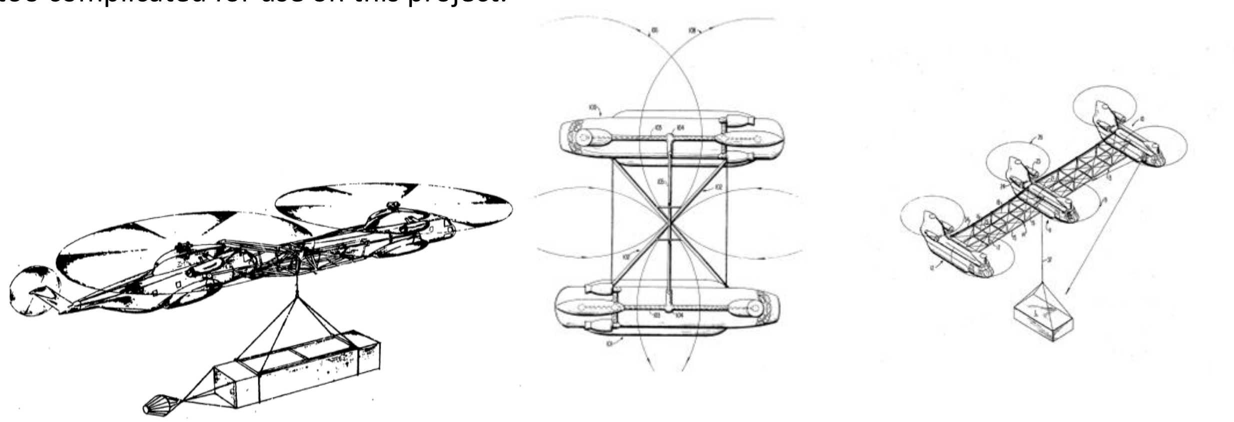

Figure 4-1: Piasecki Multi-Lift Feasibility Study (CH-53D Operational Diagram) and multi-helicopter lift patent (CH-47 transmission and connection diagram)

4.2 Pendant

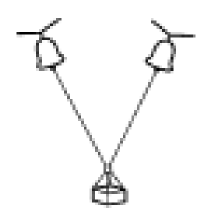

Figure 4-2: Multi-Helicopter Pendant Configuration

The pendant configuration refers to a configuration in which multiple helicopters lift a load with only tether cables. The helicopters must maintain safe separation distances through pilot control. This configuration is the cheapest solution, as other than the operational costs of the aircraft, only the cost of the required cable lengths are needed. This design is also simple as no modification to either of the aircraft is needed.

Safety is a significant concern with this method. Other than pilot control, no other system is used to keep sufficient distance between the lifting aircraft. Also, a portion of the thrust from the main rotors must be used to maintain proper horizontal spacing. As a result, vertical thrust for lift may be significantly reduced, depending on tether lengths. Due to the serious safety concerns associated with this configuration, it was discarded.

4.3 Spreader Bar

Similar to the pendant design, tethers are used to connect the load to the helicopters. However, to maintain horizontal separation, a spreader bar is used between the two tethers. The force to keep the helicopters safely at a preset separation distance is applied purely as a compressive load on the spreader bar. The helicopters are able to use the entirety of their thrust for lift and maneuvering.

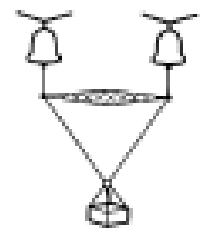

Figure 4-3: Multi-Lift Helicopter Spreader Bar Configuration

The system is relatively simple as it requires no significant modification to either helicopter. Flight characteristics are similar to both a single helicopter carrying a slung load and a single helicopter attached to a fixed anchor. The spreader bar method was chosen for this project due to its lower complexity compared to the rigid method, and its greater safety compared to the pendant method.

5 Demonstrator Aircraft Selection

Eight different aircraft were originally chosen as potential demonstrator aircraft due to their use in slung load operations. The eight models were: The Kaman K-Max, Bell/Boeing V-22, Sikorsky S-64, Sikorsky S-92, Boeing-Vertol CH-47, Sikorsky CH-53, AgustaWestland EH-101, and the Sikorsky UH-60.

After selecting these eight airframes, a set of grading criteria was created on which each model could be compared and judged, with the highest-scoring model being chosen as the demonstrator aircraft.

One of the particular grading criteria was the useful payload each helicopter could carry. A demonstrator system that can carry a larger payload than a single aircraft could alone is the objective for this design. Therefore choosing a particular aircraft with high payload capabilities was an important consideration. The next criterion was the number of engines each airframe had. This was looked at as a type of safety factor, in which the higher number of engines meant an increased chance in saving the system should some sort of engine failure occur. The last category was the practicality of each model, which was simply the number of operating helicopters over the world. Using a more widely available helicopter would make this system easier to set-up and operate as opposed to using a rarer model.

The CH-47 scored the highest based on the criteria and was ultimately selected to be the demonstrator airframe for this design project. The CH-53 also scored well, but the rotor diameter was taken into account. The rotor diameter of the CH-47 was 60 ft, while the diameter of the CH-53 was 79 ft. This means that a spreader bar for two CH-53s would have to be larger than that for two CH-47s. This solidified the choice to use the CH-47.

With the CH-47 selected, the mission weight to carry was determined to be 35,000 lbs with the gross weight of each helicopter near 50,000 lbs. The next step was to design a structure that would be used to aid in the lifting of this heavy payload.

6 Spreader Bar Design

6.1 Structure Design Tools

The following tools were used during the course of development for the SPARCL structure.

Table 6-1: Tools used for Lifting Structure Development

Tool	Type	Use
Method of Joints	Analysis by hand	Check computational results
SolidWorks	CAD/Solid modeling	Develop solid models of structure concepts
CATIA	CAD/Solid modeling	Develop solid models of structure concepts
Abaqus	FEA	Perform analysis of structure models

6.2 Structure Design Assumptions

Several assumptions were made regarding the design characteristics and operation of the lifting structure, including:

- The multi-lift system (and thus the structure) will not be used as frequently as the individual aircraft are by themselves
- There will be sufficient time and manpower to fully inspect the lifting structure between operations
- The structure should be constructed using methods materials with a high technology readiness level and near-term availability
- The primary payload will be some variant of the commonly-used commercial ISO shipping container

6.3 Preliminary Designs

Several different structure concepts were developed, with one selected and optimized for the mission. Three different structure concepts with slightly geometries or methods of operation were developed: the Donut, the Cradle, and the Beam.

6.3.1 The Donut

The Donut began as a hollow circular structure; the design intention was to suspend the payload below the structure on cables, with another set of cables connecting the structure to the parent aircraft. The Donut was to act as an "intermediary", essentially setting up a load path between the aircraft and payload. It eventually evolved into an elliptical shape and came to be used as a "spreader bar". One advantage that was found over the course of development was the low drag exhibited by the Donut in the range of expected angles of attack.

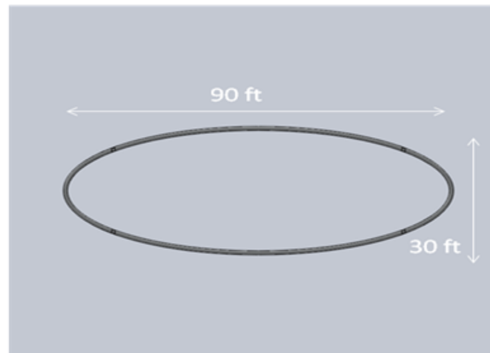

Figure 6-1: Donut Dimensions

The Donut suffered from very high weight relative to its load-carrying capacity, a trait that its low drag could not make up for.

6.3.2 The Cradle

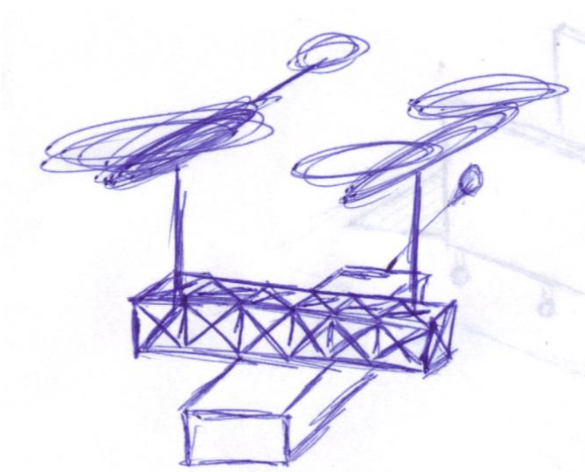

Figure 6-2: A hand drawing of the Cradle concept

The Cradle was a truss structure that operated differently from the other two concepts, in that the payload was rigidly attacked to it. One potential advantage of this arrangement was the simplicity of the dynamics of operation, i.e. having a single-pendulum system instead of a double-pendulum system as associated with the use of a spreader bar.

There were two disadvantages to adopting the Cradle. One was related to the orientation of the parent aircraft. The team's preference was to have the helicopters fly side-by-side; this means that the smallest and lightest Cradle-type structure would support the intended payload (an ISO container) with the broad side in the direction of flight, increasing the drag penalty. Also, having a rigidly-connected payload works well for an ISO container, but makes adapting other payloads for carriage difficult.

6.3.3 The Beam

The Beam is a pure embodiment of the spreader bar concept. It is a structure connected to both the aircraft and payload, primarily intended to keep the aircraft apart. It is intended to operate entirely in compression, making it a relatively simple structure. Although it could be executed in a variety of ways, the design team opted to design it as a light-weight truss. The main advantages of the spreader bar approach are light weight and payload flexibility, i.e. the ability to carry many different payload geometries with a single geometry structure.

6.4 Structure Concept Selection

The structure was selected based on a set of pass/fail criteria (*Table 6-2*). ‘Weight’ is the weight of structure, with the maximum allowable being 5,000 lbs. ‘Drag’ was a measure of the equivalent frontal area of the structure at conditions expected during the mission (to be discussed later). ‘Load-Carrying’ was the ability to lift the required 35,000 lbs payload with a safe margin. ‘Feasibility’ refers to ease of fabrication and the ability to easily take the structure apart for transport to and from mission sites.

Table 6-2: Structure Selection Details

	Donut	**Beam**	**Cradle**
Weight	Fail	Pass	Pass
Drag	Pass	Pass	Pass
Load-Carrying	Fail	Pass	Fail
Feasibility	Fail	Pass	Pass

The Donut was discarded due to a variety of problems. It was the heaviest structure, with estimates suggesting it would weight 3.70 times the Cradle, and 4.7 times the Beam. Paper analysis indicated that it would not be able to handle the loads required, and even if it had been able to do so, it was never clear how it could be easily transported and fabricated.

The Cradle was a more serious choice, but it too had less than desirable characteristics. The primary problems were structural; analysis in Abaqus revealed that failure due to compression in some members occurred at roughly 75% of the maximum expected load. Results from load conditions in which the Cradle was tilted (simulating a side-slip maneuver) were also poor.

Given the shortcomings of the other two structures, it was clear that the Beam was the best choice. It is relatively light-weight, has a small frontal-equivalent area, carries the expected payload with a comfortable margin, and should be straightforward to fabricate and transport in pieces.

6.5 Design Constraints, Requirements, and Load Cases

Several requirements were set forth by the design team for the lifting structure. These include:

- Weigh under 5,000 lbs (due to gross weight limitations)
- Must support 35,000 lbs payload (based on maximum useful external load limit)
- The structure must have a relatively low drag penalty.
- A team-developed requirement is that the structure must be air-portable by one candidate aircraft.
- A spreader-bar-type lifting structure should be approximately 90 ft long to allow sufficient separation between the rotor disks of the lifting aircraft

The load cases that were performed were purely compressive, up to a load of 30,000 lbs, which exceeds the expected compressive load on the structure for a 35,000 lbs payload. Failure occurs at this condition.

The two primary load cases were pure compression with equal loading and pure compression with unequal loading. Normal flights would take place under the former condition, while an engine-out scenario would entail the latter condition.

6.6 Design Modifications and Iterations

There were several early design iterations for the Beam. They included hollow box cross-sections, C-channels, and I-beams; many of these possessed the load-bearing ability required, but were extremely heavy. Aerodynamics analysis also showed that they had very high drag at the speeds at which the twin-lift system was expected to operate. A decision was made to develop a truss to fulfill the spreader bar function with the hope that sufficient strength could be had at lower weight and drag penalties. Efforts to transition to a truss-type structure for the Beam were very successful.

6.7 Detailed Design Tools for the Beam

Two primary design tools were used in the detailed design of the Beam. SolidWorks, a widely available commercial CAD package, was used for solid modeling and weight estimation. Abaqus, a FEA package, was used for structural evaluation of the Beam.

Hand calculations were also used extensively with Abaqus, with Hibbler's *Engineering Mechanics: Statics* and *Mechanics of Materials* being the primary sources. Hand calculations were used to determine buckling failure loads were various members used in the Beam; it was found that calculations by hand were a good supplement to the results from CAD and FEM packages.

6.8 Special Materials

The Beam is composed of existing and well-tried materials. Exotic materials were purposely avoided to keep cost and development time low. Most members are composed of an aluminum alloy, 6061-T6, which has both a stiffness and yield stress that are acceptable for this application. The "pyramidal" members at the far ends of the Beam are composed of carbon-fiber (*Figure 6-3*), which possesses a higher stiffness than aluminum. This was necessary due to the higher compressive loading in those locations. The carbon-fiber members and aluminum joints will be adhered using a special adhesive, Hysol EA 9394, which is widely used in the aviation and wind turbine blade industries for composite-to-metal secondary bonds (Juska 2010).

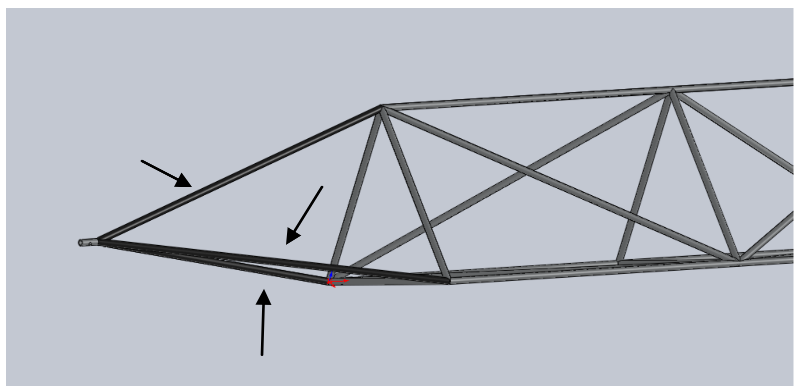

Figure 6-3: Location of Carbon Fiber Structural Members

6.9 Fabrication

6.9.1 Configuration and Structure Assembly

Overall, the Beam is 90 ft long, composed of eight 9 ft triangular cross-section "cells". These are capped by "pyramidal" structures at each end, whose members are 9.26 ft in length. The standard 9 ft cells are composed of 6061-T6 aluminum tubes with an outer diameter of 2 in and a wall thickness of 0.25 in. The pyramidal structures are composed of carbon fiber tubes with the same diameter and wall thickness.

The structure will be fabricated using existing TIG welding methods at the joints; these could present problems due to fatigue, but these issues are mitigated by the limited use of the system and the ability to fully inspect each system between operations. The entire SPARCL structure is intended to be broken down into four sections: two 27 ft long sections composed of

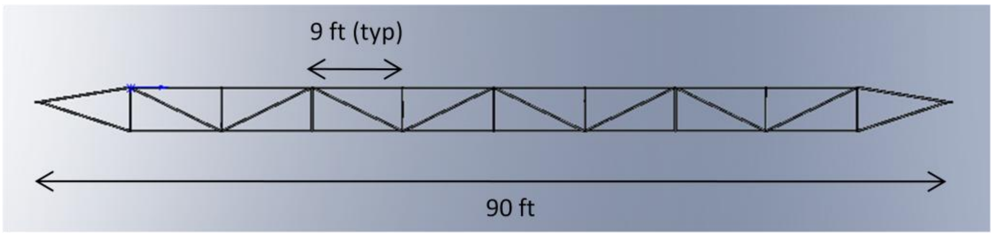

Figure 6-4: Selected Beam Dimensions

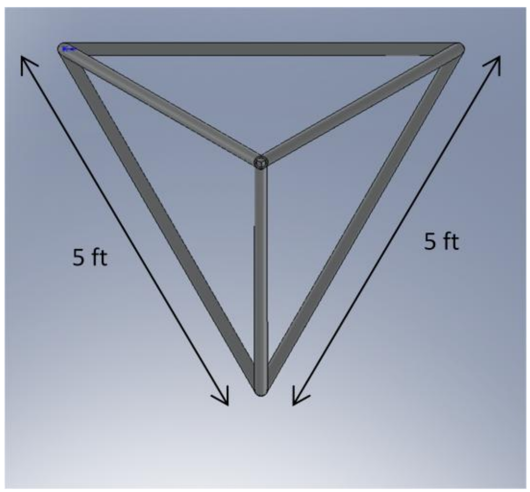

Figure 6-5: Selected Beam Member Dimensions

the outer extremes of the structure, and two 18 ft long sections composed of the inner remainder. At the joints where the structure sub-sections are connected for assembly/disassembly, the members will be secured using bolts. This allows for disassembly at the drop zone. The parts of the Beam can be loaded inside one of the helicopters for transport back to the mission start site; if time does not permit disassembly, the entire Beam can be carried as a slung-load as well.

6.9.2 Technology Readiness Level

Many of the structural components, such as the 6061-T6 aluminum alloy and the Hysol EA 9394 adhesive, are entirely off-the-shelf (OTS) components, so their TRL is quite high (on the order of

9). However, the TRL of the entire system is more important, so it cannot be said that the TRL of the entire system is as high as the individual components.

6.9.3 Cost

Overall, the cost of materials should be low. However, the structure will require some time to fabricate, and economies of scale will likely not be attainable due to the limited use of a system such as this one.

However, costs may be kept low because of the use of proven materials. Based on quotes from internet vendors, the cost for materials varied from about \$4,400.00 (“MetalsDepot”) to as much as \$7,000.00 (“OnlineMetals.com”). However, this is based on acquisition of small amounts of aluminum stock compared to the total used. Purchasing in larger bulk amounts, or purchasing in amounts custom-fabricated for this application, could reduce fabrication time and cost. Also, if welded joints are used for the aluminum sections, overall costs could be high due to the associated labor. Using adhesives exclusively could yield some cost savings while matching much of the structural performance of welds.

6.10 Cables

To connect the payload to the structure, and structure to the helicopter, there are two different concepts that could be employed: an active system that controls the motion of the load and structure, or an inactive system that connects components. Before analyzing the effectiveness of each system, the feasibility of each must be considered.

In an active system, there would be control systems that adjust the attitude of the load by adjusting the length of the cables. This would be done through winches, pulleys, and springs or shock absorbers. The feasibility of these systems is limited as most winches designed to control a heavy load are currently used in cranes and other ground based systems where the weight of the system is not a critical a parameter.

Smaller systems are used in some aircraft for maneuvering cargo, but these systems rely on wheels, pulleys, and multiples lengths of cable to reduce the weight handled. Additionally, these systems are not focused on speed of the adjustments and therefore are too slow for any practical application for dynamic adjustments in flight. A concept on the scale of the twin-lift system being developed would be complicated, have a high drag penalty, and would be too slow in operation to be practical. Therefore it is concluded that an active lifting system would be impractical, ruling it out as an option.

An inactive system is completely feasible, and could be designed around the concepts that are used in current slung load systems. The concept requires the helicopter to control the load through its static connections, and any correction in motion must be made by changes in the attitude of the helicopter. The cable lengths cannot be changed during the mission.

In an inactive control system, the geometry of the cable set up is critical in how much compression the structure undergoes and the swinging behavior of the load. These geometries depend upon the type of attachments, angle of hook ups, and the benefit of different strengths of cable. The design and material used to suspend the structure and payload below the helicopter is critical to the payload capacity of the system. Additional factors such as the weight added, drag induced, and geometry of the design are considered. The tether cables above the structure can be considered to be completely vertical to the helicopter in flight, which adds no compressive load on the structure. These attachments are designed to be a single cable from the end of the structure to the cargo hook on the helicopter.

Though CH-47 has three cargo hooks, only one is being utilized in accordance with effective loadings described by Multiservice Helicopter Sling Load: Basic Operations and Equipment. For normal external loading, the heaviest load should be attached to the center cargo hook, and the lightest on the aft hook to not hinder forward flight. Normal practice when using a CH-47 is to utilize the center hook as much as possible, and most heavy loads are rigged only to the center hook with additional lines run to other hooks for load stabilizing.

The use of only the main center hook allows for there to be more dynamic freedom for the cable. With only one hook-up, there is no moment exerted on the helicopter due to the motion of the load, and there is no possibility that a leading or trailing stabilizing cable becomes slack in flight. The design is mechanically and dynamically simple.

The bridle cables below the structure will add a compressive load to the spreader bar structure in hover, and they will extend both forward and inboard of the structure to the modeled dimensions of a 40 ft ISO container. *Figure 6-6* shows the system, and *Table 6-3* is a listing of the various tensions in the cable at each height calculation. These calculations are based on a payload of 35,000 lbs and an ISO container of 8 ft x 8 ft x 40 ft.

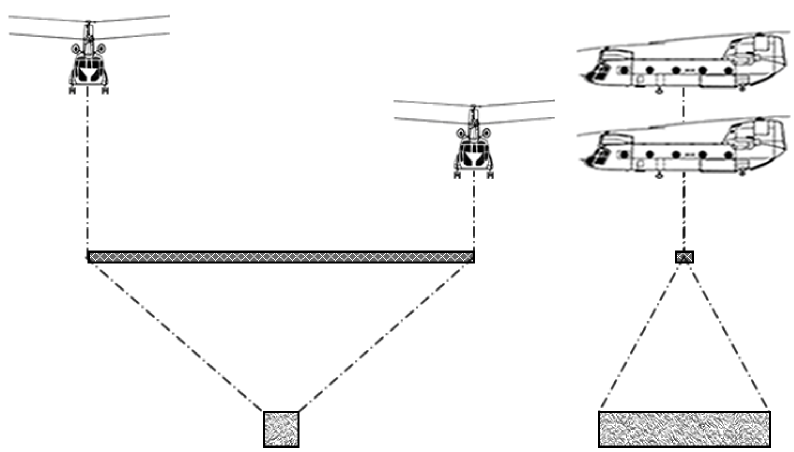

Figure 6-6: Cable Tension Geometry

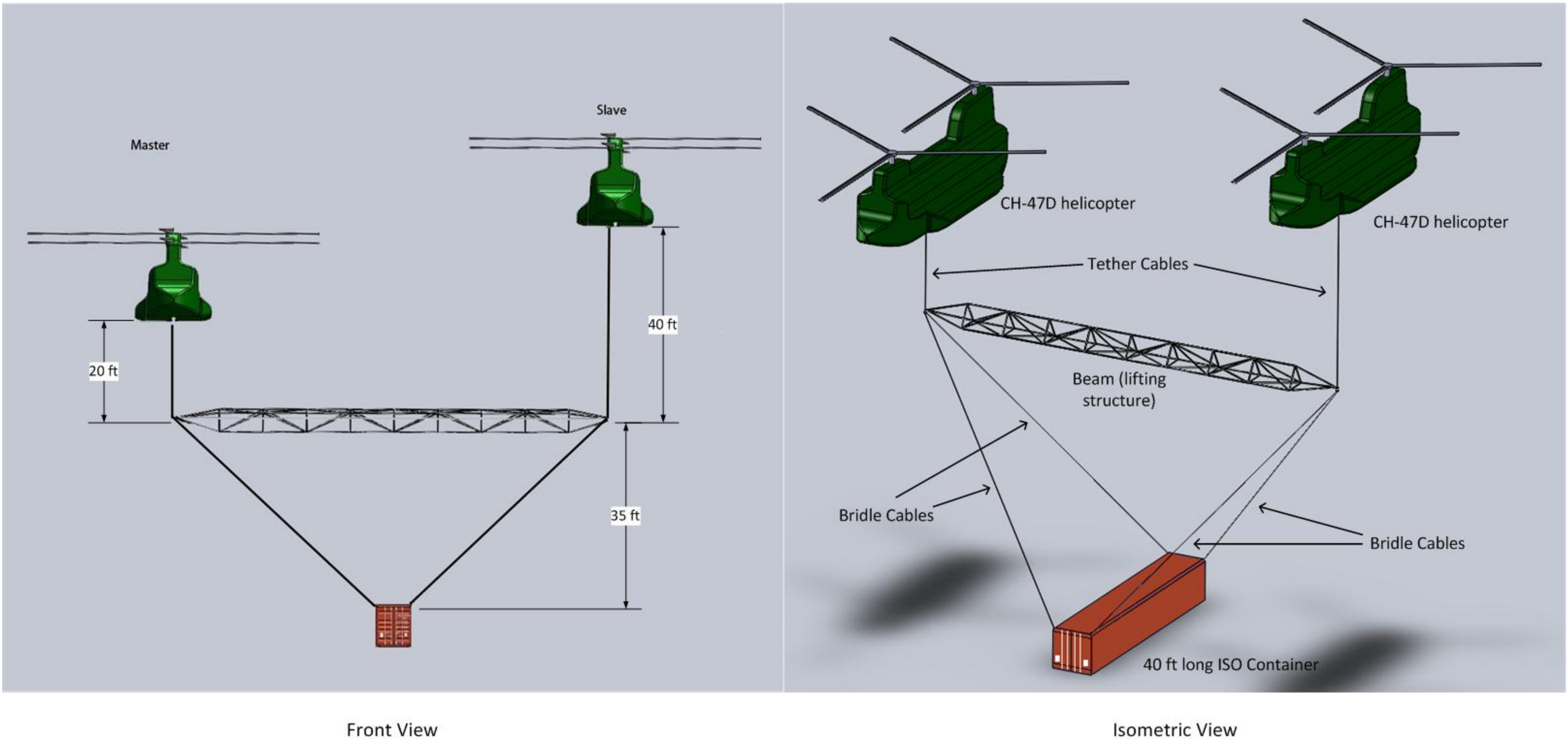

Figure 6-7: SPARCL System Diagram

Table 6-3: Compression loads associated with various load heights

Height of Load (ft)	Tension in cable (lbs)	Length of Cable (ft)	theta	phi	*Static Compression Loading*	*Total Compression Loading*
1	400000	46	1	3	400000	*419000*
5	80000	46	7	14	79000	*98000*
10	41000	47	14	27	40000	*58600*
15	28000	48	20	37	26000	*44600*
20	22000	50	26	45	20000	*38600*
25	18000	52	31	51	15000	*33600*
30	16000	55	36	56	13000	*31600*
35	14000	57	40	60	11000	*29600*
40	13000	61	44	63	9300	*27900*
45	12000	64	48	66	8100	*26700*
50	12000	68	51	68	7600	*26200*
55	11000	71	53	70	6600	*25200*
60	11000	75	56	72	6200	*24800*
65	11000	79	58	73	5900	*24500*
70	10000	84	60	74	5100	*23700*
75	10000	88	61	75	4800	*23400*
80	10000	92	63	76	4600	*23200*
85	10000	96	64	77	4300	*22900*
90	10000	101	66	77	4100	*22700*
95	10000	105	67	78	4000	*22600*
100	10000	110	68	79	3800	*22400*
1000	8800	1001	88	89	400	*19000*

The height of the load is very critical in the total compression on the structure, and therefore is the variable that can be adjusted depending on the critical buckling load of the structure. Additionally, the cables extending to the helicopter from the structure are able to add an additional compression load to the structure in dynamic loading.

To analyze the added compression force due to dynamic loading, the limitations of the system were evaluated to find what the maximum inboard angle about which both helicopters could rotate before a part would fail. The load limit of the center cargo hook is the limiting factor. The center hook is designed for a maximum normal load of 26,000 lbs, therefore, the upper cables cannot exceed 26,000 lbs in tension at any time during flight.

With the helicopters being able to move apart from one another, there are limits on the angle the helicopters can move inboard because of the maximum loading on the center hook. The maximum inboard angle is 48.3° from horizontal at the structure before altitude would be lost, or the center hook would take damage. This angle is seen in *Figure 6-8* as Θ. At this angle, there is 18,592 lbs of compression imposed on the structure.

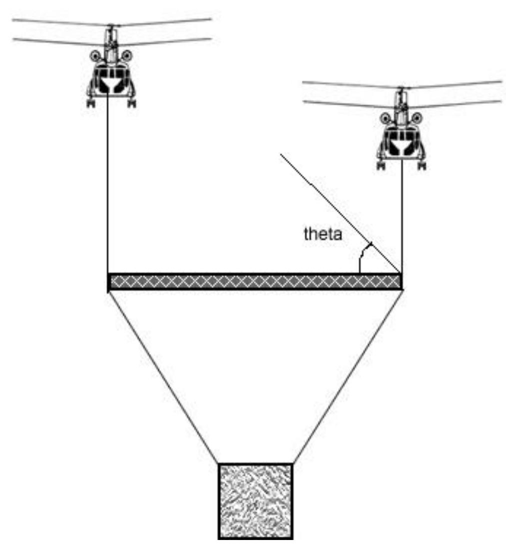

Figure 6-8: Upper cable inboard limits

The structure overall is analyzed to have a critical buckling load of 30,000 lbs. This load consists of the load from the angle of the cables below the structure, and the added dynamic loading from the helicopters both at their maximum inboard angle. Removing the possible dynamic loading, the maximum static loading capable is 21,408 lbs. As evident in *Table 6-3*, the height of load from the structure at minimum can be 20 ft. The load is designed to be slung at a height of 35 ft to leave 10,000 lbs of compression for dynamic loading and the effective increased weight during climb. The maximum rate of climb possible due to the limits of the structure and the load slung at this height is 64.4 ft/s.

The material of the cable affects multiple aspects of the performance, and the standard material used is steel cable in a variety of weaves. In the possibility of maximizing performance with a lighter weight or better dynamic material, the following other materials/products were analyzed: Twin-Path Sling, Nylon straps, Polyester loops, and Cushion-Pac® 18 a performance steel cable. These materials were compared at the given height of the load and are displayed in *Table 6-4*. The standard steel cable is found to be the best option in decision of the weight added to the system, and with consideration of the drag being based on the diameter of the material used, the steel cable again is the best for drag (*Table 6-4*).

Table 6-4: Cable Properties

Material	Diameter (in)	Total Lower Cable Weight (lbs)
Twin-Path Sling	3.00	126.40
Steel Wire IWRC	0.50	115.00
Nylon Strap	6.00	689.96
Polyester Loop	1.40	207.00

The Cushion-Pac® 18 cable is a performance compacted steel cable designed to improve performance and safety by being rotationally resistant while holding a load. For the upper cable attachments where there are single cables going from the structure to the helicopter, the maximum loading is 26,000 lbs. This will call for a 9/16 in cable diameter, which is rated for up to 38,000 lbs, and the lower cables will use a 0.5 in diameter which will are rated for up to 30,000 lbs, which will allow for the maximum rate of climb of 64.4 ft/s.

6.11 Attachment Configuration

The attachment equipment for the entire twin-lift system was configured to be easily accessible, easily assembled, and flexible for a variety of missions. There are multiple components that comprise the attachment configuration.

The first component is the tether cable that runs from each helicopter to the spreader bar. This cable will be equipped with a reach tube, for easy attachment to a hovering helicopter (*Figure*

6-9: SPARCL System Rigging). The process for attaching the structure to the helicopter will be similar to the method used to attach a load to a single helicopter in normal military sling-load operations. A hook-up man on the ground will use the reach tube to attach the cable to the center hook of each helicopter while the helicopters are in hover.

The next component is a 25 klbs-rated apex hook (*Figure 6-9C*) that will attach the tether cables with the two bridle cables and the Beam. This hook is secured with a locking pin. This allows easy disassembly of all of the cables and rigging equipment for storage and mobility purposes. This apex hook is used to attach a cable to the harness of a load in normal sling-load operations. This apex hook possesses the same load limits as the center hook on the CH-47.

The attachment configuration to the load will consist of one apex and one eye hook. The eye hook (*Figure 6-9B*) will allow for a variation load types. It will allow hookups to not only a ISO container, but also any type of harness or rigging. When picking up an ISO container, there is a solid steel loop adapter (*Figure 6-9D*) attached to the four screw locks of the container. These provide a fast and easy method of attaching cables with eye hooks to the container. A final configuration of the hookup points is shown in *Figure 6-9*.

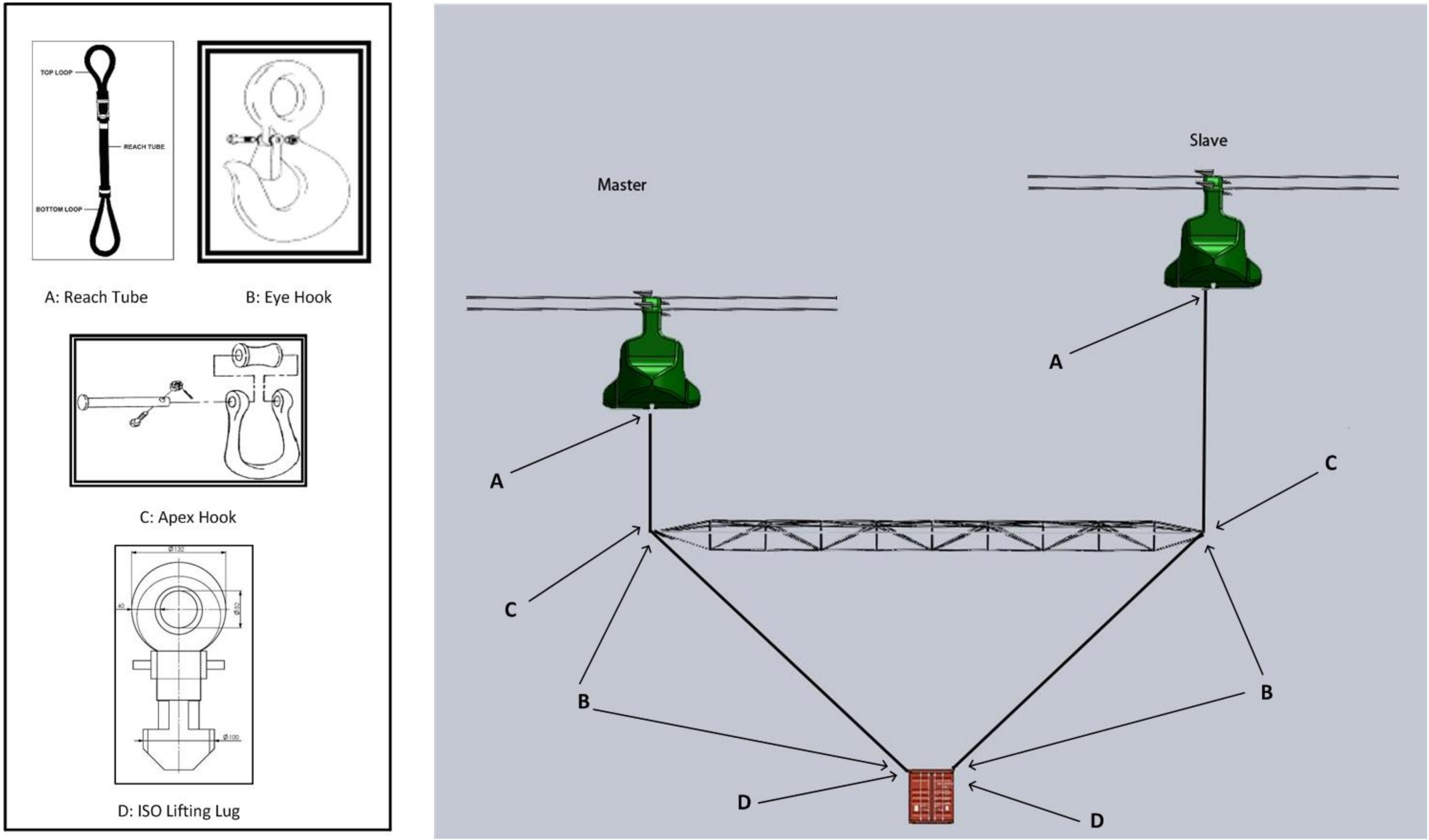

Figure 6-9: SPARCL System Rigging

7 Drag

The earliest stages of maximizing aerodynamic efficiency on the connecting structure for the twin-lift system involved finding a list of drag coefficients for various cross-sectional geometries. This allowed for the structures team to modify existing designs to include members with smaller drag coefficients.

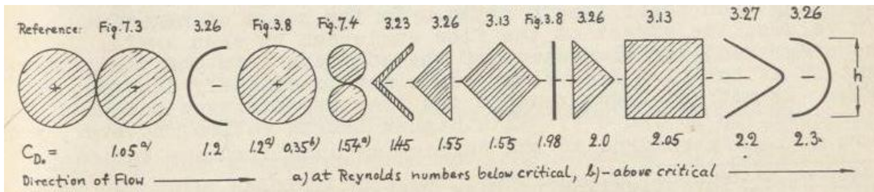

Figure 7-1: Drag Coefficients for Common Geometries (Hoerner)

The data in *Figure 7-1* were used to modify the original Beam design to include the diamond cross-section, as opposed to a square with its leading side normal to the flow (*Figure 7-2*). The Donut design and Cradle design already had circular cross-sections, and couldn't be improved upon using just this data. The Beam eventually evolved into a truss structure with relatively low-drag circular cross-section members.

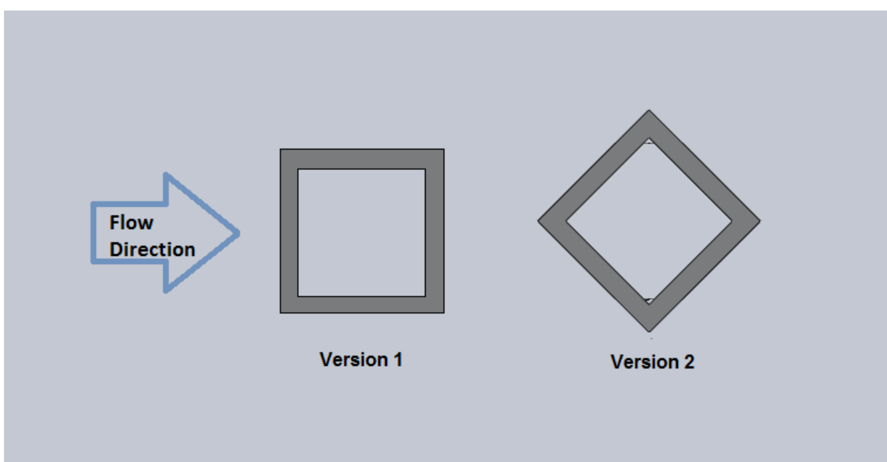

Figure 7-2: Improvement of Original Beam Design Using Aerodynamics Data

The next stage of maximizing the aerodynamic properties of the structure was to obtain a drag estimate from SolidWorks Flow Simulation. Using SolidWorks Flow Simulation provided consistent and useful results much faster than hand calculations. The initial results were compiled by running several different simulations at different flow speeds and then averaging the drag areas obtained. This was to compensate for inconsistencies in the simulation's results, but after tests for all three candidate structures were run, it became apparent that results were consistent from simulation to simulation. This led to the conclusion that only a single simulation was necessary to obtain drag data.

Because a negative angle of attack would produce a negative lift force, flow simulation was also used to output forces in the vertical direction. For these forces, a negative value would indicate a down-force, and a positive value would indicate a lift force. From here forward, vertical forces will be referred to as "lift," however most values are negative, indicating a downward aerodynamic force. Drag and lift numbers are represented as a drag or lift area, which is the force divided by the dynamic pressure of the flow. Representing drag in this fashion allows for calculation of drag and lift forces across a range of atmospheric conditions.

$$A_d = \frac{D}{\frac{1}{2}\rho U^2}$$

Equation 7-1: Drag Area

For structures where lift and drag have a strong correlation with angle of attack (i.e. they can be modeled with a function), the equations found graphically can be used to find an expression for lift at a given speed.

$$A_l = \frac{L}{\frac{1}{2}\rho U^2}$$

Equation 7-2: Lift Area

This is necessary in situations where drag would cause a change in the orientation of the structure, which would then cause a change in the aerodynamic characteristics of the structure. From a free body analysis of the structure, Equation 7-3: Alpha as a function of speed, can be obtained.

To solve for drag at a given speed, the first step is to solve the polynomial equations from the graphs, where A_d is the equation for drag area, and A_l is the equation for lift area. For the second step, the value for angle of attack that was solved for is then plugged into the equation for A_d to get the actual drag area at a given speed.

$$\frac{A_d(\alpha)}{\tan\alpha} - A_l(\alpha) = \frac{W}{\frac{1}{2}\rho U^2}$$

Equation 7-3: Alpha as a function of speed

Once this process had been developed, the Beam design was selected over the Donut and Cradle. The process of deriving drag and lift at different angles of attack began. For the Beam design, it was important to determine drag at different orientations because of swing. The drag data could then be used to find the structure orientation with the least drag.

The analysis began at an orientation where the triangular cross-section was pointed into the direction of the flow, and the orientation was varied in increments of 5° from zero to negative 60°. *Figure 7-3* shows the starting orientation and which direction is positive and negative. The structure was rotated in the negative direction.

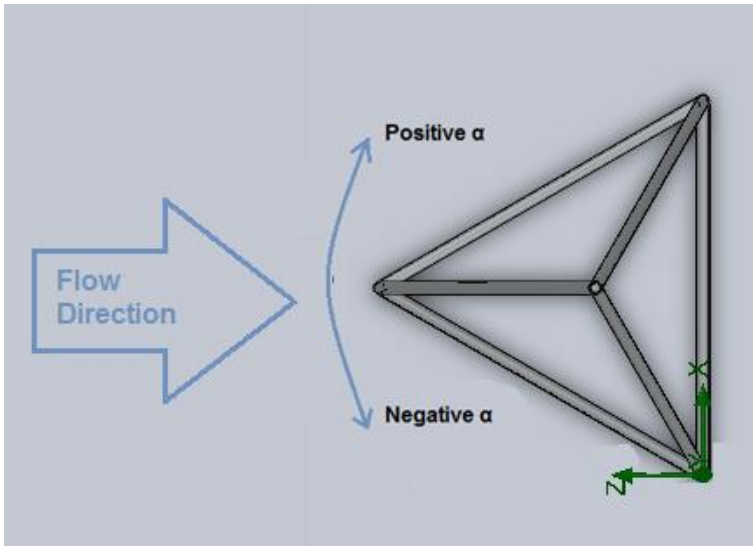

Figure 7-3: Beam Orientation

The analysis at varying angles of attack yielded the result that angle of attack doesn't have a predictable effect on drag. Drag varies very little with orientation, with maxima at about 120 ft^2 and minima at around 100 ft^2. This is probably because the truss structure is mostly open space with many small members whose orientations change relatively quickly with angle of attack.

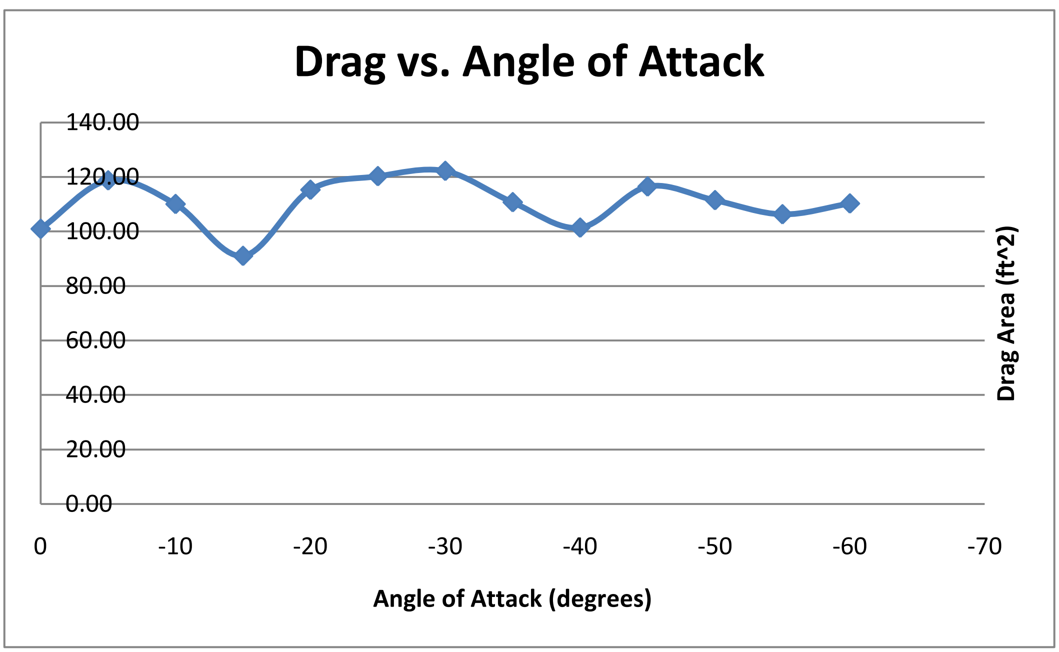

Figure 7-4: Beam Drag vs. Angle of Attack

The average value for drag area is about 110 ft^2, with of about ±10 ft^2. The maximum value is at 122 ft^2 and the minimum is at 91 ft^2. Fitting a function to the data would be difficult, and probably would not act as good model.

A hand calculation for drag area was performed by utilizing member dimensions and drag coefficients and summing the calculate drag areas. Equation 7-4: Hand Calculation of Drag can be used for this operation, where C_d is the drag coefficient for a cylinder, D_i is the diameter of a given member, and L_i is the length of a given member.

$$A_d = \sum C_d D_i L_i$$

Equation 7-4: Hand Calculation of Drag

The resulting drag area from hand calculation was 153 ft^2, which is 43 ft^2 larger than the drag area found through flow simulation. This discrepancy is likely due to the fact that the hand calculation assumes that all members are perpendicular to the flow, but many are at different angles relative to the flow. Because they are at different angles, their projected area is smaller which would result in lower drag. Also, members at an angle would have a different cross-section with respect to the flow, and thus a different drag coefficient than that used in the calculation.

Looking at lift area vs. angle of attack, there is a similar situation to that with lift. Values fluctuate between two extremes for the first 25° of rotation. This trend changes at around -30° angle of attack, where a distinct bucket-shaped curve appears with a highly negative lift area at around -45°. This prominent pattern indicates that the latter orientation should be avoided during the operation of the twin-lift system.

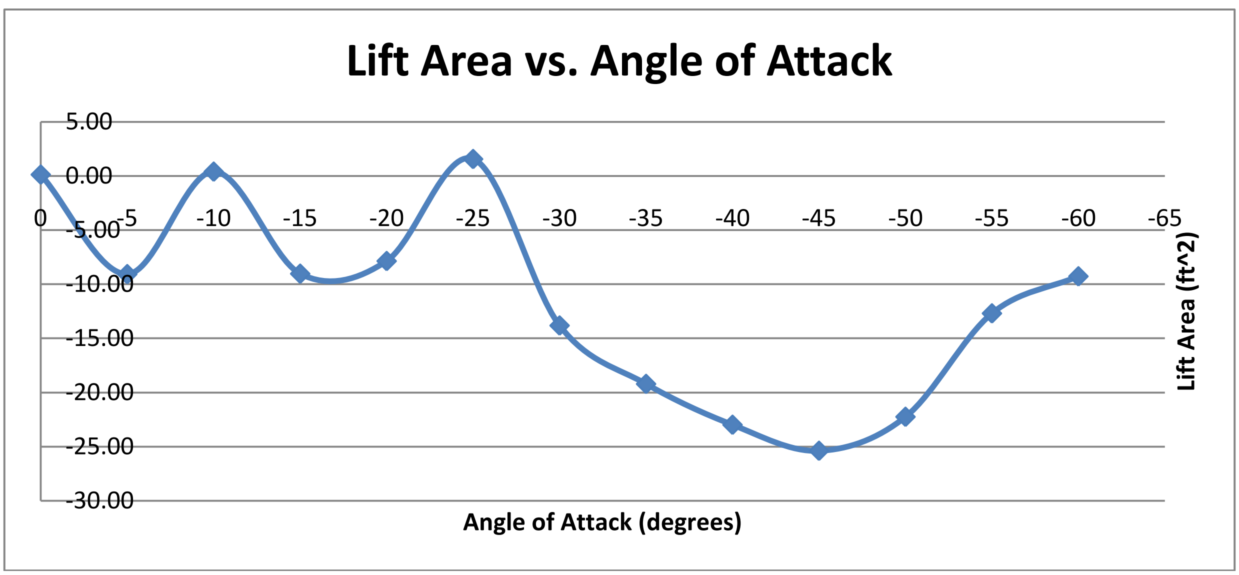

Figure 7-5: Beam Lift Area vs. Angle of Attack

After a cable analysis utilizing drag data and cable lengths, a chart of structure swing versus speed was made. According to this data, the structure would only swing 10° aft at a cruising speed of 125 kts on the return trip without the payload. This small change in orientation makes the change in both drag and lift extremely small, which makes the equation for drag at a given speed unnecessary. Though this has led to the realization that drag and lift variation with angle of attack can be neglected, this does not make the drag and lift versus angle of attack data useless. This data can be used to find the best orientation for the structure during the mission. The data indicates that an orientation with the triangular cross-section pointing into the wind (see *Figure 7-3*) has the lowest aerodynamic loads, and has little variation if the structure were to swing aft in flight.

Along with the drag calculations, the idea of adding drag-reduction mechanisms such as fairings were explored, however the added weight and complexity of such systems negated their utility. Also, fairings large enough to cover the entire structure introduced a greater drag penalty than the structure alone.

8 Dynamic Analysis

8.1 Tether length

An appropriate tether length was required for adequate safety of the twin lift system. Too long of a tether length and the two helicopters may drift into each other resulting in a catastrophic accident. Too short of a length and the structure is in danger of hitting the helicopter and the cable may be subjected to higher tensile forces during lateral displacement of the helicopters. Using unequal tether lengths allows for the safety of both the structure and helicopters. This ensures enough tip-to-tip and tip-to-body clearance between each helicopter.

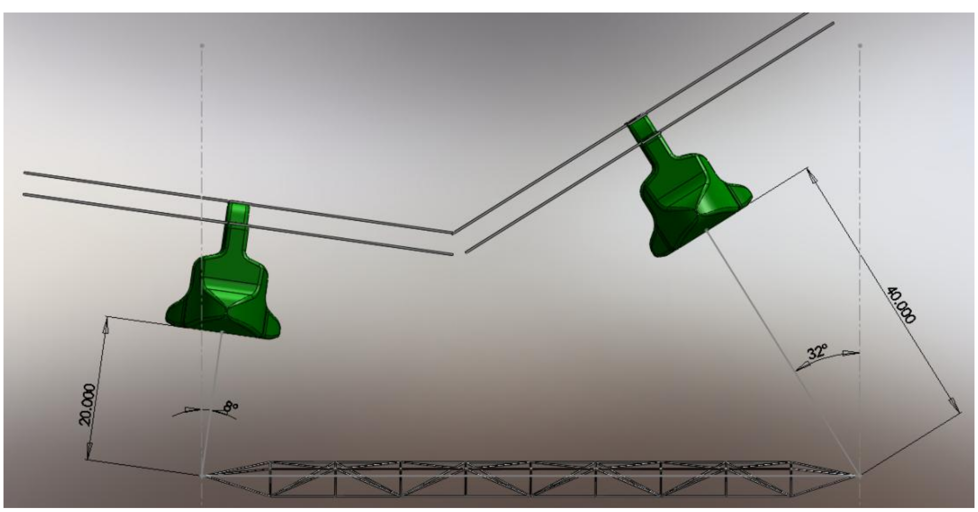

Figure 8-1: Maximum Bank Angles (Rotor Tip Limited)

Figure 8-1: Maximum Bank Angles (Rotor Tip Limited) illustrates the angles required to cause a rotor collision. However, from the Operators Manual, the pilot of a CH-47 at maximum gross weight with external loads is not permitted to bank the aircraft more than 26˚.

In a technical report written by Keath H. Reynolds of Arizona University, it was stated that the unequal tether system requires less control actions to maintain stability of the system and is safer than equal tether system due to increased rotor tip separation. *Figure 8-2*: Reynolds, 1992. Tether Length Affects On Cyclic Pitch shows one time response from Reynolds' report that compares cyclic pitch control for both tether configurations. The unequal tether graph demonstrates that the cyclic pitch is more stable and for both the slave and master aircraft.

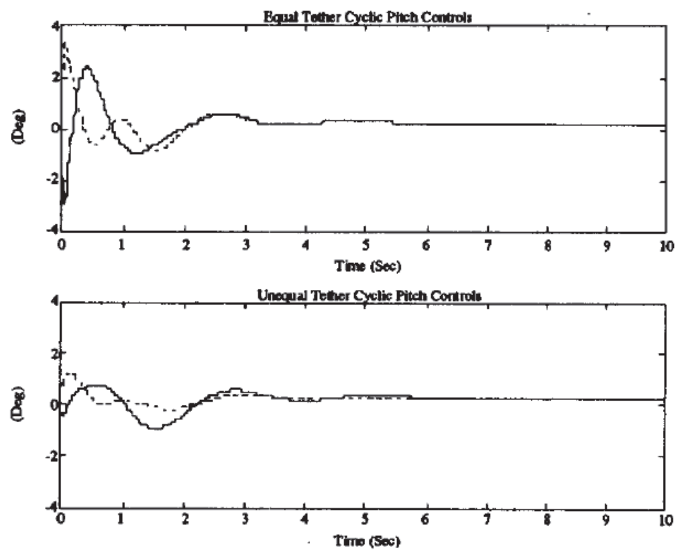

Figure 8-2: Reynolds, 1992. Tether Length Affects On Cyclic Pitch

Also a consideration was the center hook load limit of the aircraft, as the maximum allowable load on the center hook is 26,000 lb. Small horizontal deviations of the helicopter with respect to the spreader bar produces a much more significant increase in tensile force on shorter cables than with longer cables.

A slung load on a helicopter acts as a pendulum while in forward flight. The angle that it swings makes a limit for the motion of the helicopter. In the twin-lift system, there is a double pendulum with the first mass being the structure, and the second being the payload. An analysis is done to determine what kind of aft swing the load will undergo in forward flight and in forward accelerating flight.

In forward flight, the load must be examined at a range of cruise speeds that the system may undergo. For this analysis, speeds from 3 to 101 kts were examined to understand how much swing will be seen after acceleration and into the cruise speed. The motion can be simplified, where L_1 will be either 20 or 40 ft depending on which aircraft, and L_2 will be 35 ft. Thirty-five feet is used instead of the actual length of the cable because 35 feet is the effective height at which the load is designed to be slung.

The equations of motion are formulated as shown in *Table 8-1.*

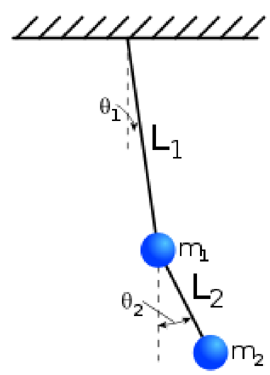

Figure 8-3: Double Pendulum Dynamics

.

Table 8-1: Double Pendulum Formula

Upper Angle	Lower Angle
$\theta_1 = \sin^{-1}\left(\frac{-2\,D_{Structure}}{3\,W_{Payload}\,L_1 g}\right)$	$\theta_2 = \sin^{-1}\left(\frac{-2\,D_{Payload}}{W_{Payload}\,L_2 g}\right)$

Acceleration is included by adding in a forward thrust force into the model with the drag in the equations, and these are all calculated and shown in *Table 8-2.* The thrust is modeled at 0.5g for forward acceleration.

Table 8-2: Pendulum Angles

Forward Speed (knots)	Single Pendulum		Double Pendulum			
	Steady Flight (degrees)	Acceleration (degrees)	Deflection under constant forward flight speed (degrees)		Deflection under 0.5 g acceleration (degrees)	
			Theta 1	Theta 2	Theta 1	Theta 2
3	0.01	6.56	0.00	0.00	18.28	1.07
9	0.06	6.61	0.04	0.01	18.32	1.08
15	0.16	6.71	0.11	0.02	18.40	1.09
21	0.32	6.87	0.22	0.04	18.51	1.11
27	0.53	7.08	0.37	0.06	18.67	1.13
33	0.79	7.35	0.55	0.10	18.86	1.16
39	1.11	7.66	0.76	0.14	19.09	1.20
50	1.89	8.46	1.31	0.23	19.66	1.30
56	2.36	8.93	1.63	0.29	20.01	1.36
62	2.88	9.46	1.99	0.35	20.39	1.42
68	3.46	10.05	2.39	0.42	20.82	1.49
74	4.09	10.68	2.83	0.50	21.28	1.57

This data clearly show how the behavior of the load is critically important on the payload, and much less on the weight of the structure. This can also be modeled as a single pendulum as also shown in

Table 8-2. These numbers are different, because of different ways of analyzing the motion of the pendulum and the inherent complexities of a double pendulum. These values show how the expected aft swing of the load will be between the values found. Forward acceleration however can be expected to behave only like the values found for the lowest speeds, as this is acceleration, which will be when coming from a stop. The greatest swing anticipated is around 20° for initial acceleration, and this will settle down to less than 10° during the cruse portion of the flight.

The system as a whole behaves in two different stages. The initial stage with the greatest aft swing will occur for a short time only during the initial acceleration of the system. At cruse the system will settle to a more neutral state where all the attachments will play the biggest role in the drag of the system during the cruse portion of the flight where the speed is the greatest.

8.2 Hover Dynamics

The stability and control of the lift system is important in the safety and operation of the mission. A system that will compensate for any instabilities and ease pilot workload is necessary for the success of the mission. Our analysis focused on the lateral stability of the lift system during hover. In 1982, H.C. Curtiss and F.W Warburton published a study on longitudinal stability of a twin lift system, and their paper*, Stability and Control of the Twin Lift Helicopter System*, became a basis for our study. The entire system has seven degrees of freedom, each helicopter has two translational and one angular degree of freedom and one degree of freedom is required to describe the load motion.

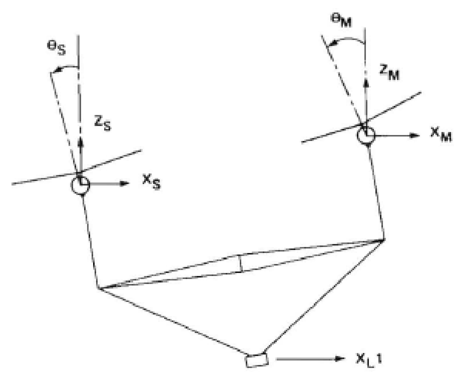

Figure 8-4: Degrees of freedom for THLS

Notation

(B_{lc})-A_{lc} = helicopter cyclic control
e_b = spreader bar inertia parameter
g = gravity constant
H_1, H_2 = tether length, unequal
H_A = average tether length
h' = vertical separation between helicopter CG and tether attachment point, ft. (positive below CG)
I_x (I_y) = helicopter moment of inertia, slug-ft^2
I_B = spreader bar moment of inertia
K_A, K_D = attitude feedback gains
L = spreader bar length, ft
M_B = spreader bar mass, slugs
M_H = helicopter mass, slugs
M_L = payload mass, slugs
M_u ($-L_v$), M_q (L_p), X_u (Y_v), Z_w = stability derivatives
S = non-dimensional parameter, measure of tether length difference
W_L = load weight
W_H = helicopter weight
ω_H = load pendulous frequency
ω_H = uncoupled frequency associated with Δz

$x(-y)$	= horizontal displacement of helicopter CG, ft, parallel to spreader bar
x_l	=load displacement with respect to space, ft
x_l'	= load motion coordinate, ft
$X_{Blc}(Y_{Alc})$, $M_{Blc}(-L_{Alc})$, $Z_{\theta c}$	=Control derivatives
Z	= vertical distance from spreader bar to load CG, ft
Z	= vertical displacement of helicopter CG, ft
ϵ	$=M_H h'/I_y$, ft^{-1}
ϵ^*	$= \epsilon_b + 4\mu\delta_L(1-\delta_L)\hat{Z}^2$
Θ_c	= helicopter collective control, rad
δ_L	$=M_L/M_L+M_B$
μ	= mass ratio, $M_L + M_B/2M_H$
$\theta(-\phi)$	=angular displacement of helicopter, rad
$\Sigma(\ )$	= sum coordinate, Equation 8-1: Sums and differences of displacements
$\Delta(\ )$	= difference coordinate, Equation 8-1
$(\hat{\ })$	= length normalized by L
$(\ )_m$	= master helicopter
$(\ )_s$	= slave helicopter

The sums and differences of the displacements of the master and slave helicopters for the lateral case are defined below:

$$\Sigma Y = \frac{Y_m + Y_s}{2} \qquad \Sigma\theta = \frac{\theta_m + \theta_s}{2} \qquad \Sigma Z = \frac{Z_m + Z_s}{2}$$
$$\Delta Y = Y_m - Y_s \qquad \Delta Z = Z_m - Z_s \qquad \Delta\theta = \theta_m - \theta_s$$

Equation 8-1: Sums and differences of displacements

We first sought to replicate Dr Curtiss' findings for a given example longitudinal case using a script we had produced in Matlab. Terms include longitudinal displacement (X), lateral displacement (Y), vertical displacement (Z), roll (ϕ, radians), pitch (θ, radians). We've reproduced the equations of motion:

$$[M]=\begin{bmatrix}(1+\mu) & 0 & 0 & 0 & 0 & 0 & 0\\ 0 & 1 & 0 & 0 & 0 & 0 & 0\\ 0 & 0 & 1 & 0 & 0 & 0 & 0\\ 0 & 0 & 0 & 1 & 0 & 0 & 0\\ 0 & 0 & 0 & 0 & 1 & 0 & 0\\ 0 & 0 & 0 & 0 & 0 & 1+e_b & 0\\ 0 & 0 & 0 & 0 & 0 & +4\mu\hat{Z}^2\ \delta_L & 0\\ 0 & 0 & 0 & 0 & 0 & x(1-\ \delta_L) & 0\\ 0 & 0 & 0 & 1 & (h'+H_l) & \delta_L\hat{Z} & 1\end{bmatrix}\quad [C]=\begin{bmatrix}-Z_w & 0 & 0 & 0 & 0 & 0 & 0\\ 0 & -X_u & 0 & 0 & 0 & 0 & 0\\ 0 & -M_u & -M_q & 0 & 0 & 0 & 0\\ 0 & 0 & 0 & -X_{uw} & 0 & 0 & 0\\ 0 & 0 & 0 & -M_u & -M_q & 0 & 0\\ 0 & 0 & 0 & 0 & 0 & -Z_w & 0\\ 0 & 0 & 0 & 0 & 0 & 0 & 0\end{bmatrix}$$

$$[K]=\begin{bmatrix}0 & 0 & g(1+\mu) & 0 & 0 & 0 & 0\\ 0 & \mu\omega_A^2 & +\mu\omega_A^2 h' & 0 & 2\mu\omega_A^2 H_l S & 0 & 2\mu\omega_A^2\\ 0 & \epsilon\mu\omega_A^2 & \epsilon\mu\omega_A^2(H_A+h') & 0 & 2\epsilon\mu\omega_A^2 H_l S & 0 & 2\epsilon\mu\omega_A^2\\ 0 & -\frac{\mu}{2}\omega_A^2 S & -\frac{\mu}{2}\omega_A^2 h'S & 0 & g(1+\mu S\frac{H_l}{H_A}) & 0 & -\mu\omega_A^2\\ 0 & -\frac{\mu}{2}\epsilon\omega_A^2 S & -\frac{\mu}{2}\epsilon\omega_A^2 h'S & 0 & \epsilon\mu\omega_A^2 H_l S & 0 & -\epsilon\mu\omega_A^2\\ 0 & -2\mu\ \delta_L\hat{Z}\omega_A^2 S & -2\mu\ \delta_L\hat{Z}\omega_A^2 h'S & 0 & -4\mu\ \delta_L\hat{Z}H_l\omega_A^2 & 4\mu\ \delta_L\hat{H}_A\hat{Z}\omega_A^2 & -4\mu\ \delta_L\hat{Z}\omega_A^2\\ 0 & \frac{1}{2}\omega_A^2 & \frac{1}{2}\omega_A^2 Sh' & 0 & \omega_A^2 H_l & 0 & \omega_A^2\end{bmatrix}$$

$$[B]=\begin{bmatrix}1/2Z_{\theta_c} & 1/2Z_{\theta_c} & 0 & 0\\ 0 & 0 & X_{B_{1s}} & -X_{B_{1s}}\\ 0 & 0 & M_{B_{1s}} & -M_{B_{1s}}\\ 0 & 0 & 1/2X_{B_{1s}} & 1/2X_{B_{1s}}\\ 0 & 0 & 1/2M_{B_{1s}} & 1/2M_{B_{1s}}\\ Z_{\theta_c} & -Z_{\theta_c} & 0 & 0\end{bmatrix}$$

$$M\ddot{x}+C\dot{x}+Kx=Bu$$

Equation 8-2: Matrices, Equations of motion for longitudinal hover

The system as a whole is maneuvered by collective and collective cyclic. Helicopter spacing is controlled by differential cyclic. There are two motions that describe the basic motions of the system, anti-symmetric and symmetric shown by *Figure 8-5*. Equal collective pitch of both helicopters only results in vertical translation of the whole system. Equal cyclic pitch on both helicopters produces an anti-symmetric motion where the helicopter separation distance and relative roll are maintained ($\Delta\dot{Y}=0$ and $\Delta\varphi=0$). The system rotates ΔZ and translates $\Sigma\dot{Y}$. Equal and opposite cyclic pitch will produce symmetric motion but will not rotate or translate the entire system. The master and slave helicopters will only move with relation to each other.

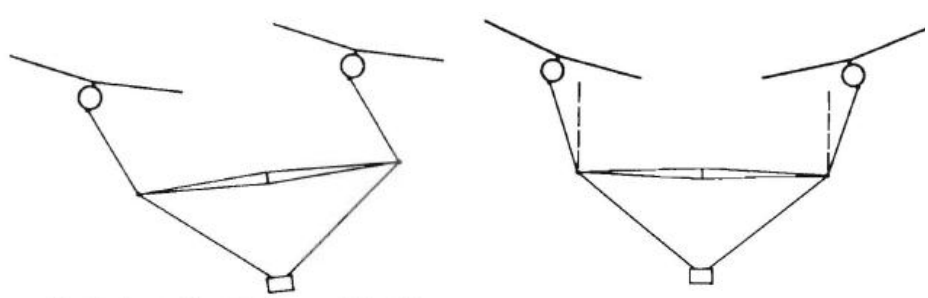

Figure 8-5: Anti-Symmetric and Symmetric Motion

From Dr. Curtiss' analysis it was concluded that divergence becomes very fast the further below the attachment point is from the helicopter's CG (*Figure 8-7*: Dr Curtiss: Variation of symmetric modal characteristics with increasing tether attachment point -cg spacing (μ =0.45). *).* He concludes that for the tether to be attached to the bottom of the fuselage, feedback control is required. (μ = mass ratio, M_L+M_B/2M_H)

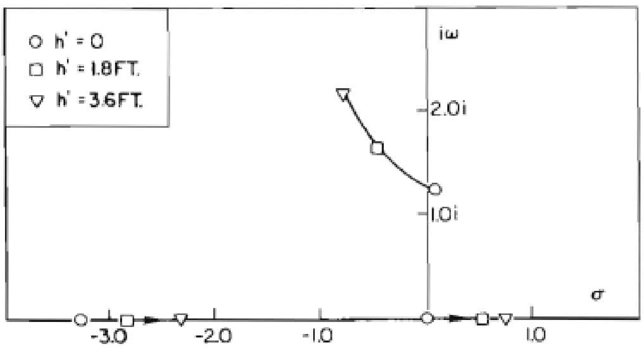

Figure 8-7: Dr Curtiss: Variation of symmetric modal characteristics with increasing tether attachment point -cg spacing (μ =0.45).

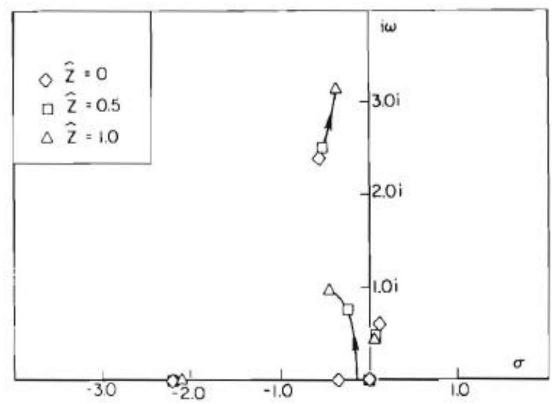

Figure 8-6: Dr. Curtiss: Variation of anti-symmetric modal characteristics with load position with respect to spreader bar (μ =0.45).

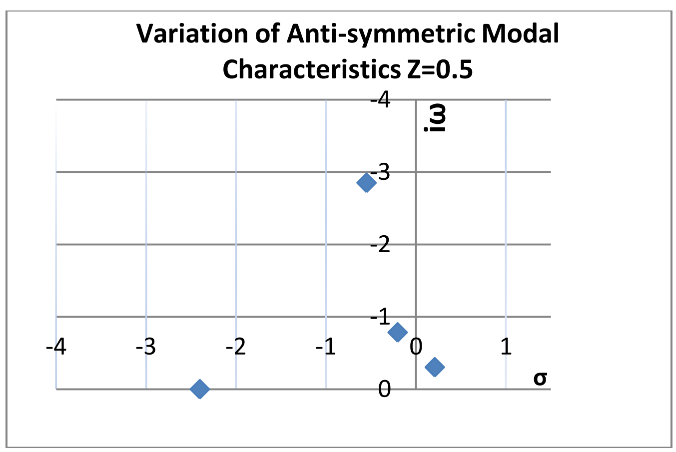

Figure 8-8: Curtiss THLS Eigenvalues of Linearized Dynamics

Once the validity of the code was verified (*Figure 8-8*) using the example helicopter parameters given in Dr. Curtiss's paper, we made the appropriate changes to convert the script from longitudinal analysis to lateral analysis and changed load and spreader bar properties to match our configuration. Stability and control derivatives for the CH-47 at v= 0.1 kts, SAS on, were obtained an Ames Simulation report (Weber, 1984) and were added to the code, along with the desired tether lengths of 20 ft and 40 ft for the master and slave helicopters respectively, and distance from the load to the spreader bar of 35 ft, shown in *Figure 8-9.*

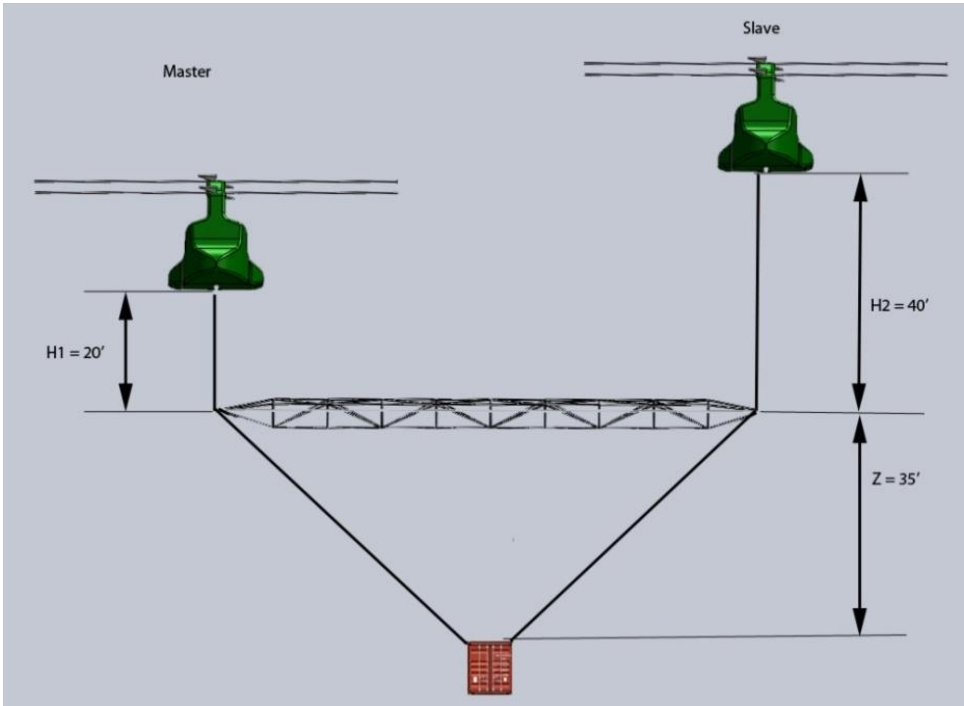

Figure 8-9: Helicopter and load configuration diagram

For this configuration, the entire system carrying a 35,000 lbs payload has the Anti-Symmetric and Symmetric Modal characteristics shown in *Figure 8-10* and *Figure 8-11* respectively. The Anti-Symmetric Modal characteristics show two unstable modes that would need to be corrected using feedback control.

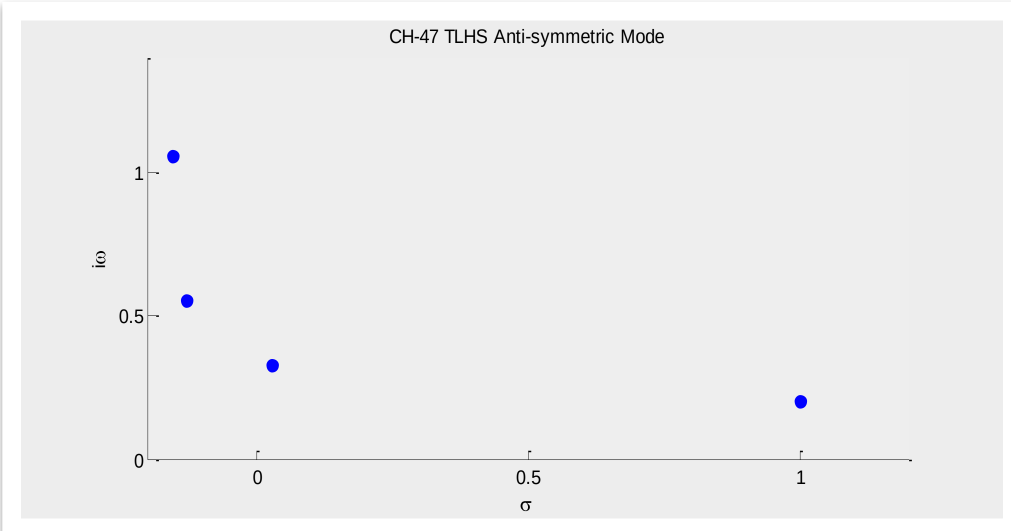

Figure 8-10: CH-47 THLS Anti-Symmetric Modal Characteristics

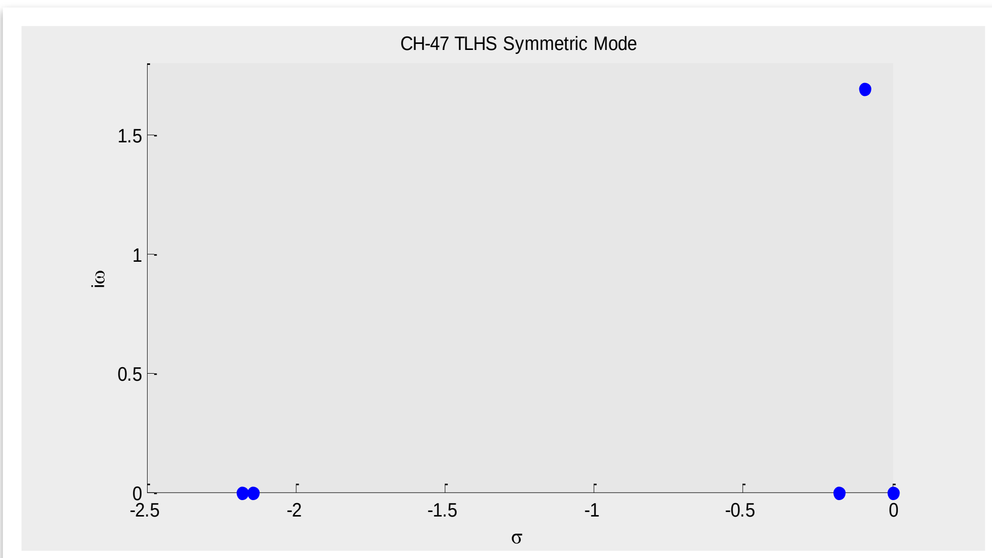

Figure 8-11: CH-47 THLS Symmetric Modal Characteristics.

Using the resulting equations of motion, we constructed an equivalent state-space system which allowed us to determine the response of the system due to disturbances in the ϕ, Z, and Y directions. For a 10° roll difference between the master and slave helicopters, the response of the master helicopter is shown in *Figure 8-14*: . Both lateral and roll movements quickly diverge to unsafe states.

Using a Linear-Quadratic Regulator (LQR), the optimal gain matrix K was computed. A new state-space model was created to incorporate the optimal gain K. The initial response of the master helicopter with the same initial disturbance with gain K is shown in *Figure 8-14.* Control is greatly improved as each divergence is dampened within 30 seconds.

The stick and collective deflection in inches needed to produce given response for the master helicopter is shown below. The Q and R matrices used in the LQR calculation were chosen to produce the desired gain that did not take too much stick deflection to accomplish. Ideally this system should only require stick deflections of less than 15% of full stick travel to ensure that not only does the system have enough control authority to perform stability maneuvers, but that the pilot is still able to perform the required mission maneuvers.

This system is shown to stabilize large disturbances within roughly 30 seconds, using minimum stick deflections. This stability system is necessary to keep each vehicle in trim safely using little or no pilot input to ease workload. This system is envisioned to be tied to the autopilot system so no hardware modifications to the flight controls would be required. However, the flight control computer would have to be updated to include this add-on.

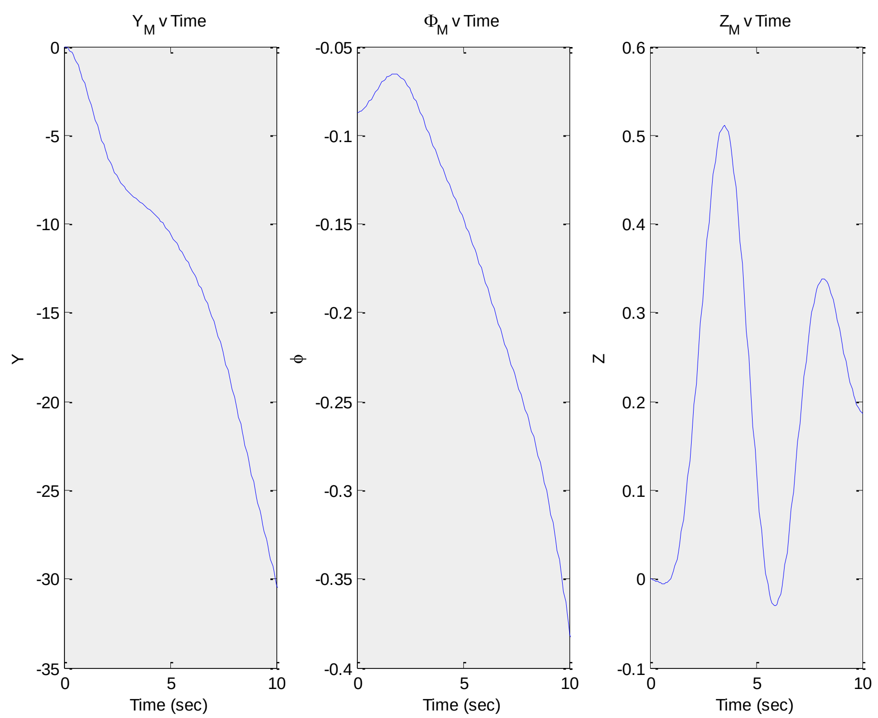

Figure 8-13: Master Helicopter with 10 degree disturbance.

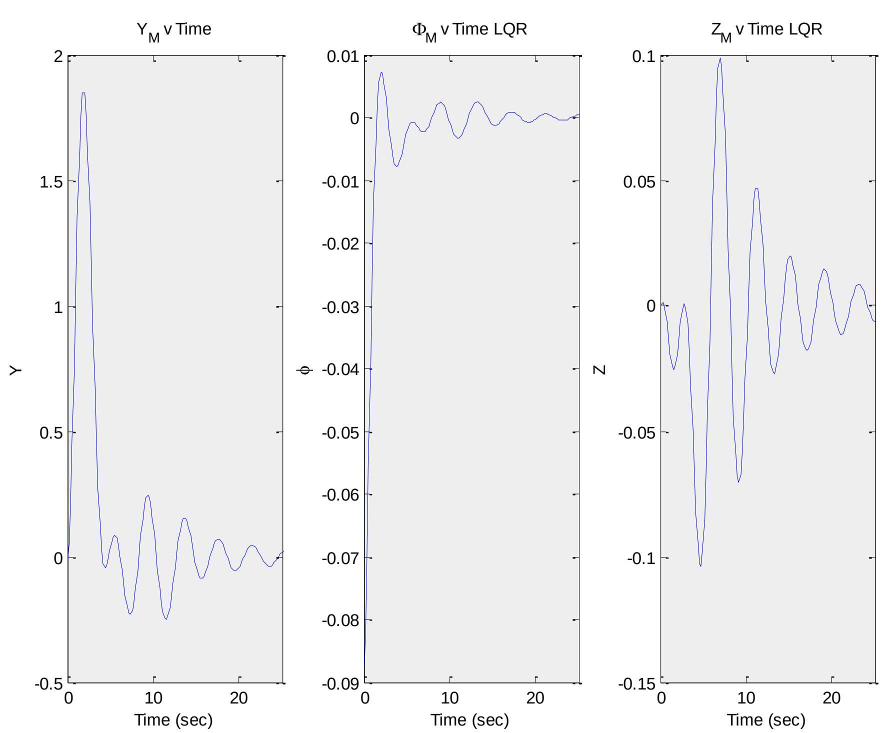

Figure 8-14: Master helicopter with 10 degree disturbance with gain K

THLS State Space Matlab Code

```
A = [zeros(7,7), eye(7); -inv(M)*K, -inv(M)*C];
D = [zeros(7,4); -inv(M)*B];

Sys = ss(A, D, eye(14), []);
```

THLS LQR Matlab Code

```
Q = diag([1,1,57.3^2,1,57.3^2,1,0,0,0,0,0,0,0,0]);
R = diag([1,1,1,1])*20;
K = lqr(A, D, Q, R);

Lsys = ss((A-D*K), [], eye(14), []);
```

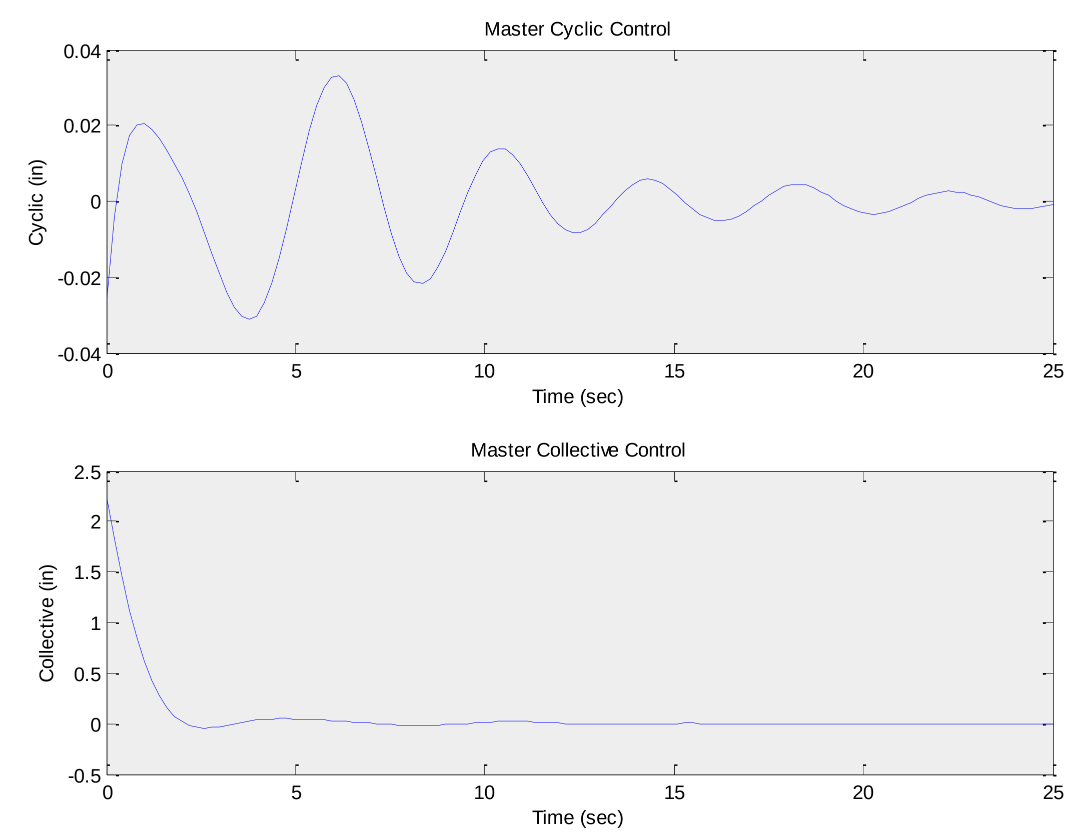

Figure 8-12: Master Cyclic and Collective Control with Gain K

9 Controls Integration

To use the LQR feedback control system, real time position data would be needed for each helicopter and for the load. Various methods and hardware would be required to measure the 14 position and velocity data ($\Sigma Z, \Delta Y, \Delta\varphi, \Sigma Y, \Sigma\varphi, \Delta Z, Y_L^{'}, \Sigma\dot{Z}, \Delta\dot{Y}, \Delta\dot{\varphi}, \Sigma\dot{Y}, \Sigma\dot{\varphi}, \Delta\dot{Z}, \dot{Y}_L^{'}$) .

To measure ΔY and $\Delta\dot{Y}$, laser range finders are needed to measure the distances between the helicopters. A GPS receiver is to be placed on the load itself to measure Y_L' and $\dot{Y}_L'$. An Air Data Inertial Reference Unit (ADIRU) and GPS systems would provide the other positional and velocity data needed for the LQR feedback system.

The LQR feedback control software would be integrated into the autopilot system as an add-on package. This is to take advantage of the control authority the autopilot has over the flight control system. Using the data from the hardware sensors, the LQR system would compute the necessary flight control movements needed to correct, if necessary, any unstable movement of the helicopter system.

This system is based on the control hierarchy of a master and slave helicopter. Each helicopter has its own flight crew, where one is designated as the "Master" helicopter, and the other, the "Slave." Both will have their own synchronized flight plan that the pilots will follow to achieve the mission specifications while the LQR system is engaged in the background with the autopilot system to actively respond to pilot deviations that produce any unstable or undesired motions. This system decreases the workload that the crews must perform to keep the two aircraft at safe distances from each other during maneuvers.

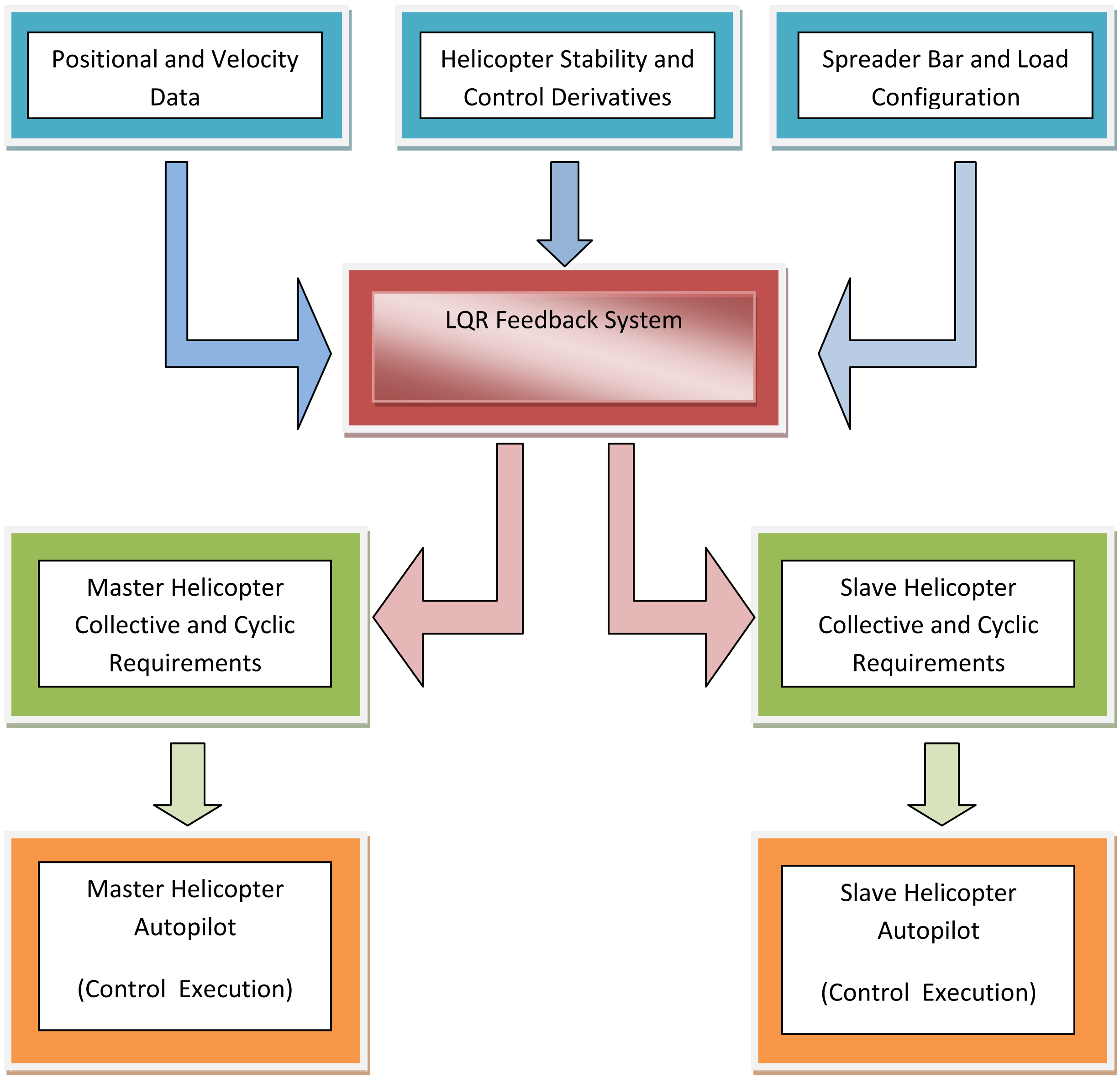

Figure 9-1: Control Integration Schematic

10 Performance

With the CH-47 chosen as the demonstrator helicopter for the mission and the selected structure complete, the next goal was to determine if the helicopter could perform the RFP mission with the structure and design load while also considering fuel consumption and airspeed. The drag area and the gross weight of the system had to be taken into consideration for each of the three legs of the mission:

- Outleg, flying 100 nm with the payload
- Hovering with the payload for ten minutes
- Returning 100 nm without the payload

To begin, performance data charts in the CH-47D Operator's Manual (TM 1-1520-240-10) were used to find not only appropriate flight speeds, but also fuel consumption for each part of the mission. The RFP indicated that the altitude for the mission was sea level and the temperature was 35° Celsius (referred to as ISA + 15°).

10.1 Outleg

To deliver the payload to the drop-off site, the twin-lift system must travel 100 nm with the payload, and because the structure and payload are external, there would be a subsequent increase in drag at forward velocity. To overcome this increased external drag area, an increase in engine torque (percentage increase) is required. The equivalent drag on one helicopter is equal to half the drag area of the structure and half the drag area on the payload. Per helicopter, the drag area of the structure was 100 ft^2, while the drag area of the ISO container was equal to 250 ft^2, so the total effective drag area per helicopter was 350 ft^2. Using *Figure 10-1*(CH-47D Operators Manual, Fig 7-8-1), drag area (Drag Area Change), true airspeed (TAS), pressure altitude, free air temperature (FAT), and additional torque required for a desired cruise speed can be found.

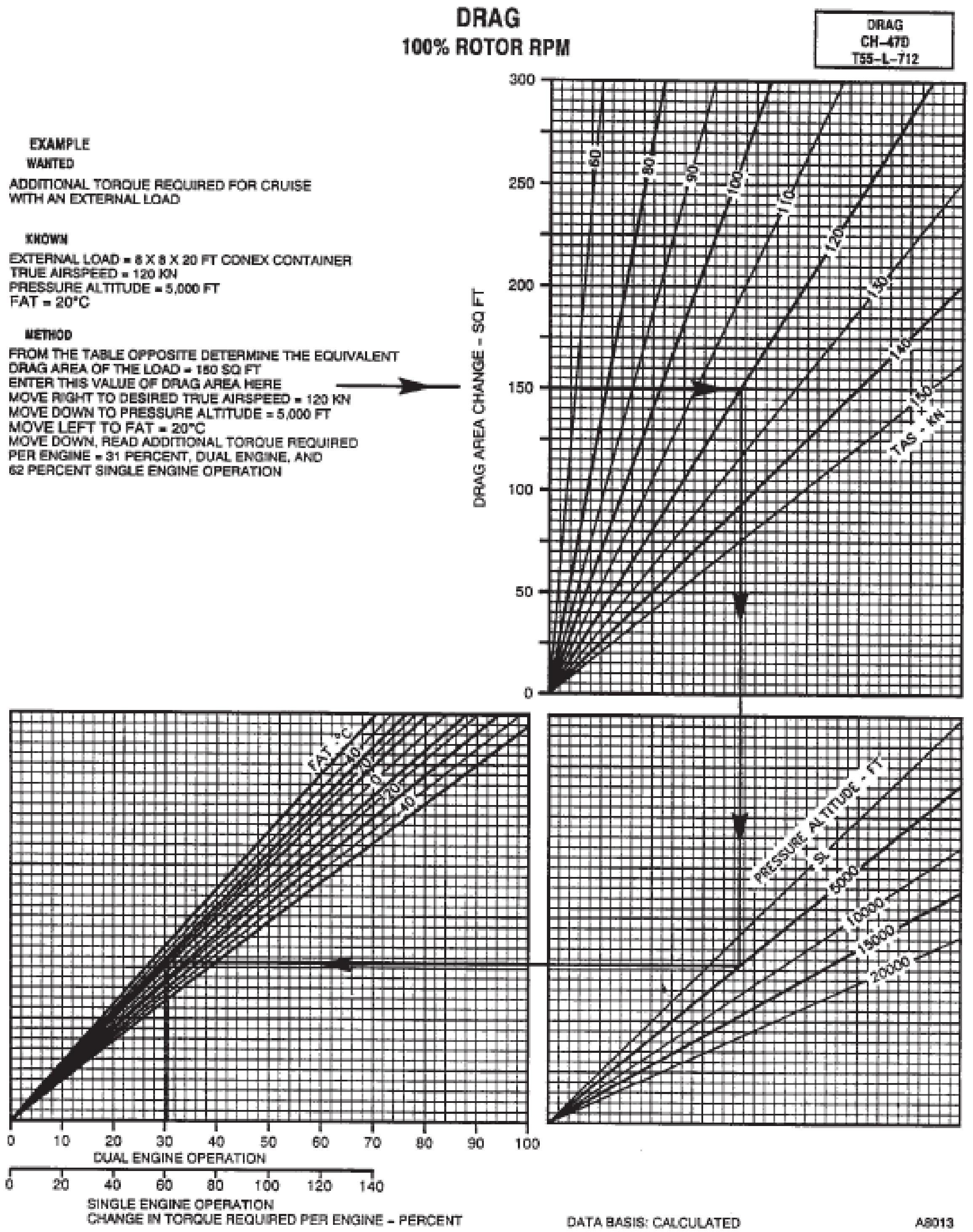

Figure 10-1: Drag area change vs. torque change

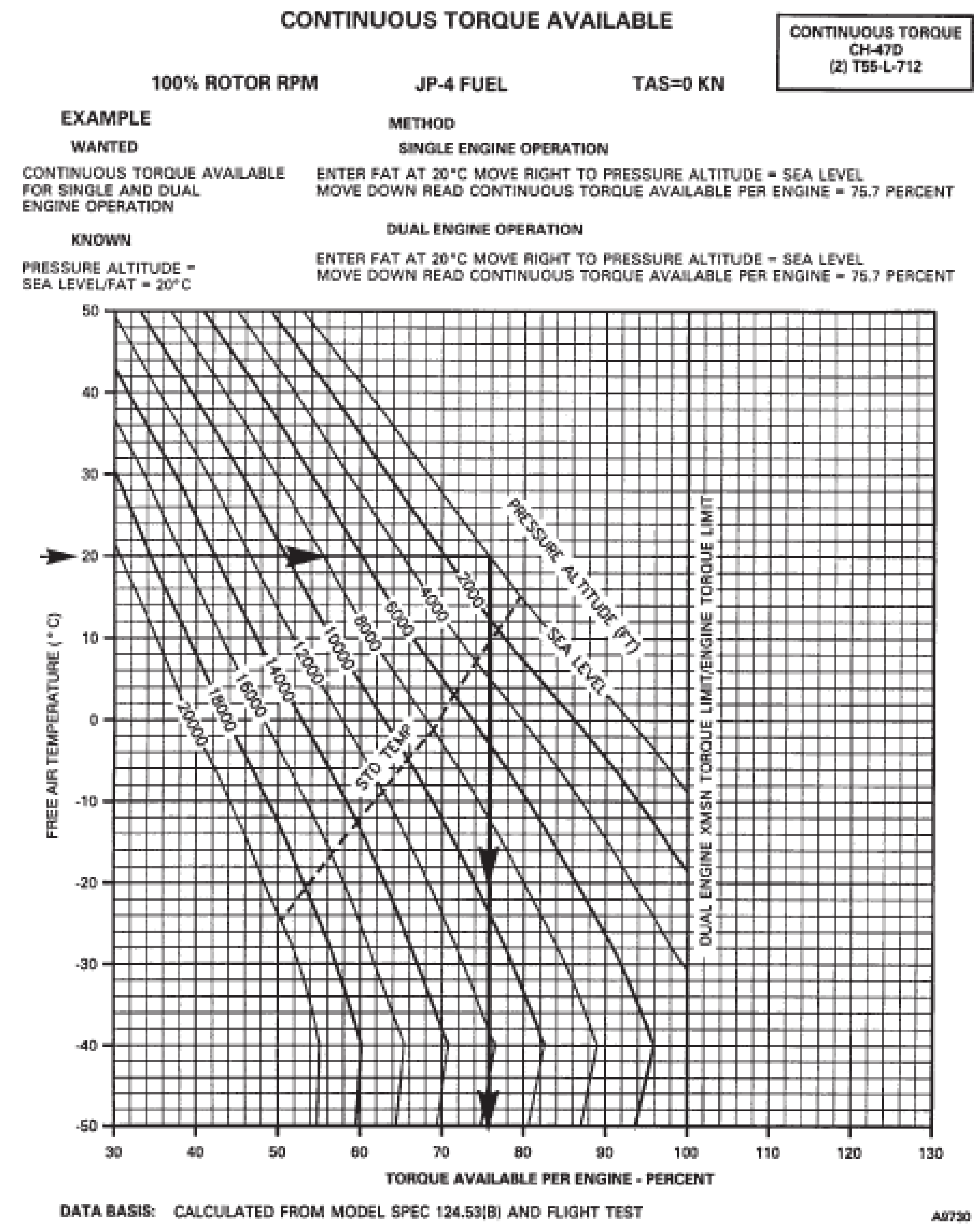

Figure 10-2: Continuous torque available

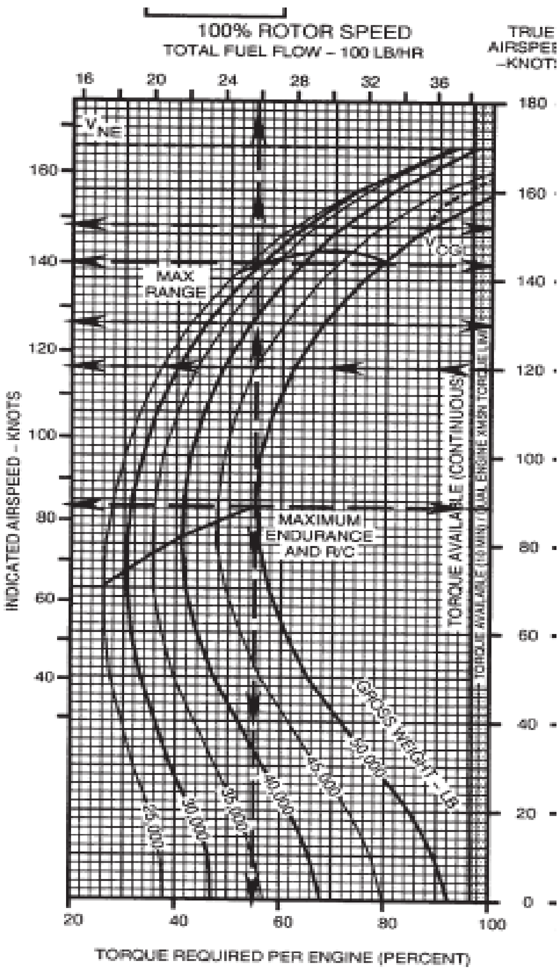

Figure 10-3: Flight speed vs. torque required

Using *Figure 10-3*, a table was created for a range of airspeeds from 50 to 100 kts in order to determine the fastest allowable airspeed the helicopters could fly at. Using the *Figure 10-3*, it is found that the max continuous torque available from the engines of the CH-47 at ISA + 15° and sea level conditions was 67%. The maximum continuous torque limit is set by a combination of the pressure altitude and FAT, and is based on engine fatigue limits. The maximum speed at which each helicopter in the twin-lift system is able to fly is limited by the maximum continuous torque; the total percentage of torque required for the system to fly at cruise speed is the sum of the percentage of torque required for the helicopter to fly at cruise speed, plus the percentage of torque required to overcome the drag area change due to the structure and payload. The total percentage of torque required must be less than 67% for normal operating conditions. Using the gross weight and the total drag area of the system, 50,000 lbs and 350 ft^2 respectively, *Table 10-1*, indicates that 70 kts was the fastest allowable speed for this leg of the mission. Applying the required engine torque to *Figure 10-4* describing torque versus fuel flow, fuel usage was also found. The fuel used per helicopter for this stage of the mission 4,077 lbs, and with a price of $3.13/gal for JP-8, fuel costs are $1,904 per helicopter.

Table 10-1: Airspeed & Fuel Usage at GTOW of 50,000 lbs

Knots	Torque	Torque Change Due to Drag	Total Torque	Max Cont. Torque	Fuel Flow (lb/hr)	Fuel Consumption (lbs)
50	63%	3%	66%	67%	2840	5680.88
55	61%	5%	66%	67%	2834	5158.39
60	59%	7%	66%	67%	2839	4741.20
65	58%	8%	66%	67%	2850	4389.37
70	56%	10%	66%	67%	2851	4076.64
75	56%	12%	68%	67%	2900	3856.73
80	56%	14%	70%	67%	2952	3689.50
85	56%	17%	73%	67%	3051	3600.18
90	57%	19%	76%	67%	3118	3461.20
95	58%	22%	80%	67%	3241	3402.88
100	59%	24%	83%	67%	3314	3314.20

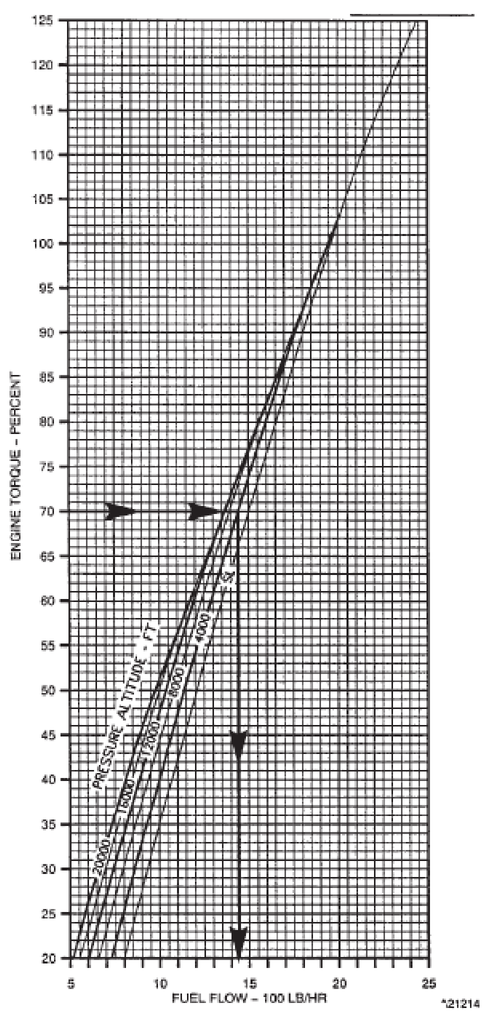

Figure 10-4: Engine torque vs. fuel flow

10.2 Hover

The twin lift system must then hover with the payload at the drop-off site for ten minutes. Using the CH-47D manual on torque required to hover (*Figure 10-5*), required torque was found to hover, and using the torque versus fuel flow (*Figure 10-4*), and fuel usage were found. To hover at out of ground effect (OGE), the fuel flow is 1,600 lb/hr, and to hover for ten minutes, each helicopter consumes 316.7 lbs of fuel, costing $145 per helicopter.

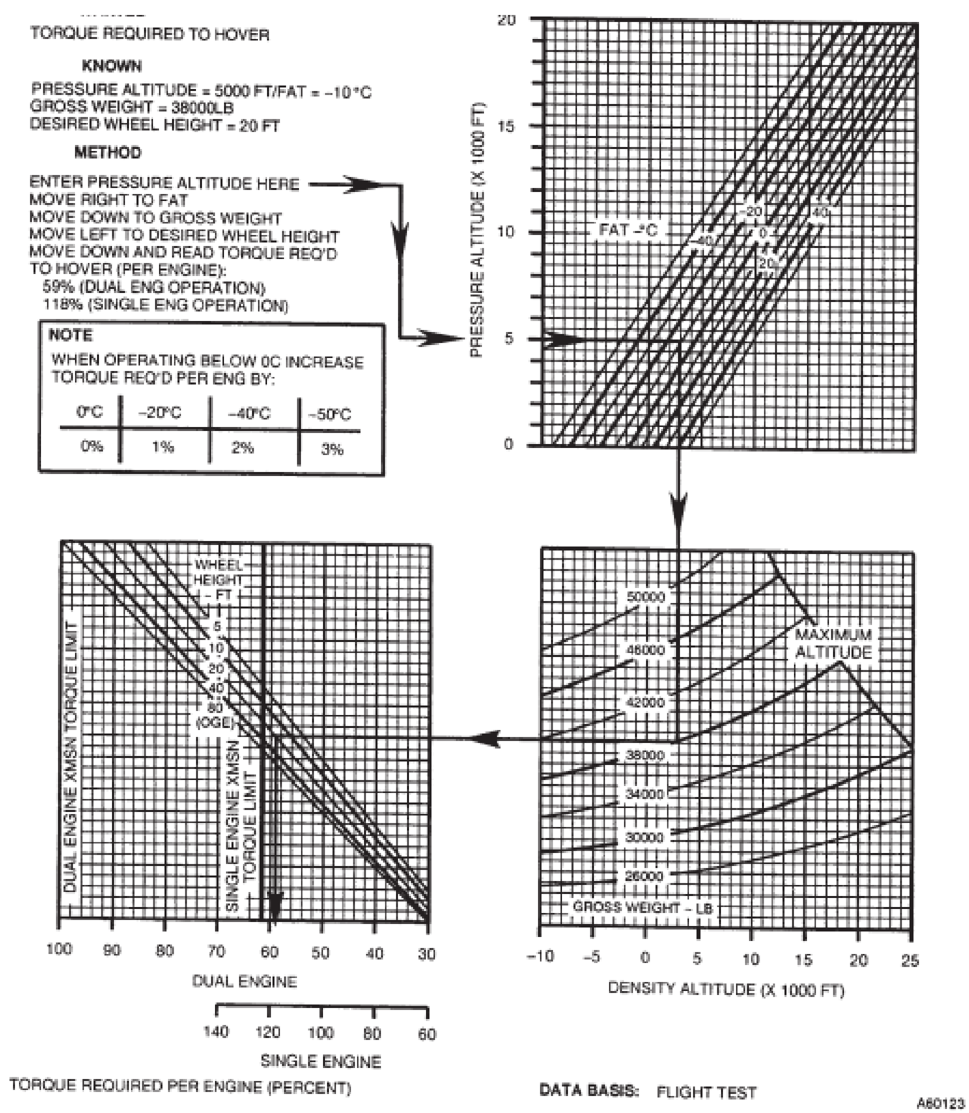

Figure 10-5: Torque required to hover

10.3 Return Trip

The final stage of the mission is to return 100 nm carrying only the structure. The drag area is reduced since the helicopters are no longer carrying the payload, and the gross weight is greatly reduced from the absence of the payload as well as the fuel that was consumed during the mission. With 4400 lbs of fuel already burned during the mission, the gross weight for each helicopter is ~ 28,000 lbs. Using the appropriate line from *Figure 10-3*, another table was generated for this leg of the mission. From the *Table 10-2*, it is found that 125 kts is the highest allowable speed for this leg of the mission, and that 2,074 lbs of fuel will be used in the process per helicopter, costing $969.

Table 10-2: Airspeed & Fuel Usage at GTOW of 30,000 lbs

Knots	Torque	Torque Change Due to Drag	Total Torque	Max Cont. Torque	Fuel Flow (lb/hr)	Fuel Consumption (lbs)
50	32%	1%	33%	67%	1737	3474.88
55	31%	2%	33%	67%	1724	3138.19
60	30%	3%	33%	67%	1722	2875.81
65	30%	3%	33%	67%	1726	2658.41
70	30%	4%	34%	67%	1748	2499.35
75	30%	4%	34%	67%	1762	2343.19
80	31%	5%	36%	67%	1807	2258.25
85	31%	6%	37%	67%	1836	2166.48
90	32%	6%	38%	67%	1868	2073.70
95	33%	7%	40%	67%	1921	2016.88
100	34%	7%	41%	67%	1959	1959.20
105	36%	12%	48%	67%	2144	2037
110	38%	13%	51%	67%	2228	2005
115	40%	15%	55%	67%	2340	2036
120	42%	17%	59%	67%	2452	2035
125	44%	20%	64%	67%	2592	2074
130	46%	25%	71%	67%	2788	2147

With the speeds and the amount of fuel used for each of the three legs of the mission accounted for, it is evident that from a performance and fuel aspect that this mission can be completed. The total fuel used throughout the mission totals 6,465 lbs. The total fuel each helicopter was carrying at the start of the mission is 7,400 lbs, leaving 935 lbs as reserve in the case of unforeseen circumstances. The total cost of fuel per helicopter is $3,457 for 7,400 lbs of JP-8, for the entire system the cost is $6,914 for the required amount of fuel per mission.

10.4 Mission Capable

Based off of the maximum gross weight (50,000 lbs), the empty weight (23,401 lbs), and the necessary fuel (7,400 lbs) for each demonstrator helicopter, the useful payload of the demonstrator aircraft 19,199 lbs. The RFP requires that the system be able to lift a payload 1.75 times the weight that a single aircraft can carry alone. The payload weight to carry based on this requirement is 33,598 lbs (19,199 x 1.75 = 33,598). Our system not only meets, but exceeds the requirement, carrying a payload of 35,000 lb plus a spreader bar weight of 1,083 lb. This leaves 2,315 lb for flight crew and other unaccounted for discrepancies.

10.5 Emergency conditions

Engine failure on one or both of the helicopters must be considered. One of the main factors in determining the performance of a helicopter with a single engine is altitude, our mission flight conditions are sea level so our system can still possibly complete the mission in case of an engine out. In the event of an engine failure the helicopter's speed must be reduced to 60 kts as stated in the CH-47D Operator's Manual, therefore the fully functioning helicopter must also slow to 60 kts. Also, the helicopter with the engine failure should not have a gross weight exceeding 46,000 lbs according to *Figure 10-6* from the Operator's Manual. The helicopters would have to reposition themselves to distribute the weight of the payload. Since the fully functioning helicopter is limited to a 50,000 lb gross weight, should the engine failure occur before 62 nm has been traveled, then the payload would immediately have to be jettisoned due to the system being overweight, or the fully functioning helicopter must operate under emergency torque conditions. Under the 30 Minute Emergency Torque Condition, the fully functioning helicopter has an available 75% engine torque, an increase of roughly 10% from normal operating conditions. Under the 10 Minute Emergency Torque Condition, the fully functioning helicopter has an available 98% engine torque. Using the emergency torque conditions it would be possible to return to the mission start site with payload if the aircraft are close enough, however emergency torque conditions will place high levels of stress on the fully functioning helicopter's engine and transmission. After the 62 nm however, the helicopters would not need to enter emergency torque conditions and would only have to alter their positions to distribute slightly more weight onto the fully functional helicopter.

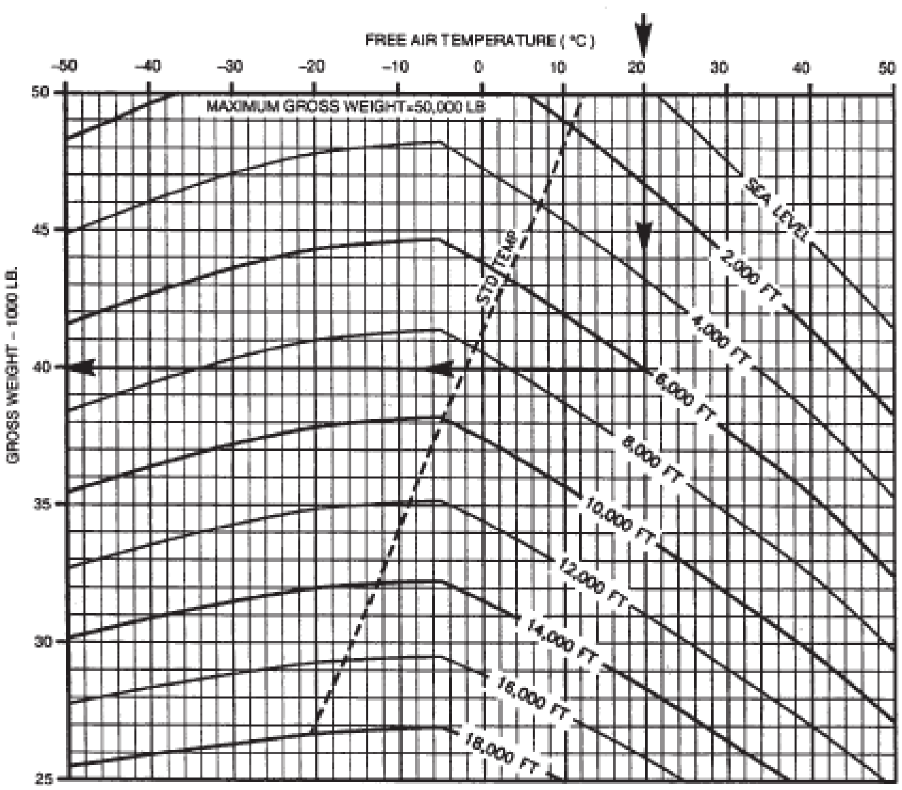

Figure 10-6: Gross Weight Allowed with Single Engine Failure

Using fuel usage tables it is determined that if the mission is still in the out-leg segment and the helicopters have traveled 83 nm or more of the required 100 nm then there would not be enough fuel on board to return to the mission start site at any point. The helicopters could fly to the drop off point and deliver the payload, and the helicopter with the failed engine would either be required to refuel or find a landing zone within 80 nm. Should the single engine failure occur during the return trip then the reserve fuel should be enough to get both helicopters back safely without complications. Should an engine fail on both helicopters during the return trip no adjustments would be made; however if both helicopters have engine failure on the out-leg trip or during hover then the structure and payload should be immediately released.

11 Operational Procedure

1. A qualified ground crew will assemble the Beam at the mission start site.

    1.1. Make sure structure has been inspected after prior flights for cracks and other fatigue or operation-related damage.

2. The Beam should be moved into position near the payload.

    2.1. The Beam does not necessarily need to be positioned *above* the intended payload. It could be placed nearby such that the helicopters will lift the structure over the payload.

3. Attach bridle cables to the payload.

    3.1. The bridle cables are attached via eye and apex hooks to the far ends of the Beam. The tether cables are attached to the same set of apex hooks.
    3.2. The bridle cables are attached to the payload via eye and apex hooks attached to ISO container-specific eye hooks. Different payloads, such as light armored vehicles, may be attached directly to the bridle cable eye hooks.

4. Attach tether cables to helicopters.

    4.1. This is performed with the helicopters hovering above the structure.
    4.2. In either case, the tether cables are connected to the center cargo hooks via reach tubes. These make attachment while the helicopter is hovering easier.
    4.3. The tether cables are attached to the Beam via eye and apex hooks.

5. The helicopters engage augmented control system, pick up payload, and accelerate to cruising speed

    5.1. Pay attention to engine torque, etc., because an accident at this stage could require aborting the mission.

6. The helicopters cruise for 100 nm.

7. The helicopters hover for 10 min at the drop-zone while depositing the payload.

    7.1. The helicopters land, disassemble the Beam, and carry the components and cables internally at this point, or attach the complete Beam as a slung-load to a single aircraft.

    7.2. As an alternative, the structure could be carried as a slung-load by a single helicopter. These operations might be performed with or without having the helicopters land, but would require transferring of cables.

8. The helicopters fly at cruising speed 100 nm back to the mission start site.

12 Conclusion

Many attempts have been made in the past to use more than one helicopter to lift a load one single aircraft could not. Currently, there is a stronger rationale than ever to pursue a twin-helicopter lift system (THLS). With the development and procurement costs of new aircraft being what they are, there are numerous cost and time incentives to use existing airframes for a super-heavy-lift mission.

The SPARCL team has developed a concept that uses a commonly available heavy-lift helicopter, the CH-47 Chinook, to demonstrate a twin-helicopter lift system. The system uses a spreader bar to keep horizontal separation between the helicopters; this spreader bar is a simple truss structure made of off-the-shelf components. Much of the cables and rigging equipment used to attach the helicopters, structure, and payload are now commonly used in the helicopter slung-load operations. As an improvement to previous THLS attempts, control concepts conceived by Reynolds, Curtiss, and Warburton have been used to develop an augmented control system that lowers pilot workload significantly and uses largely existing hardware.

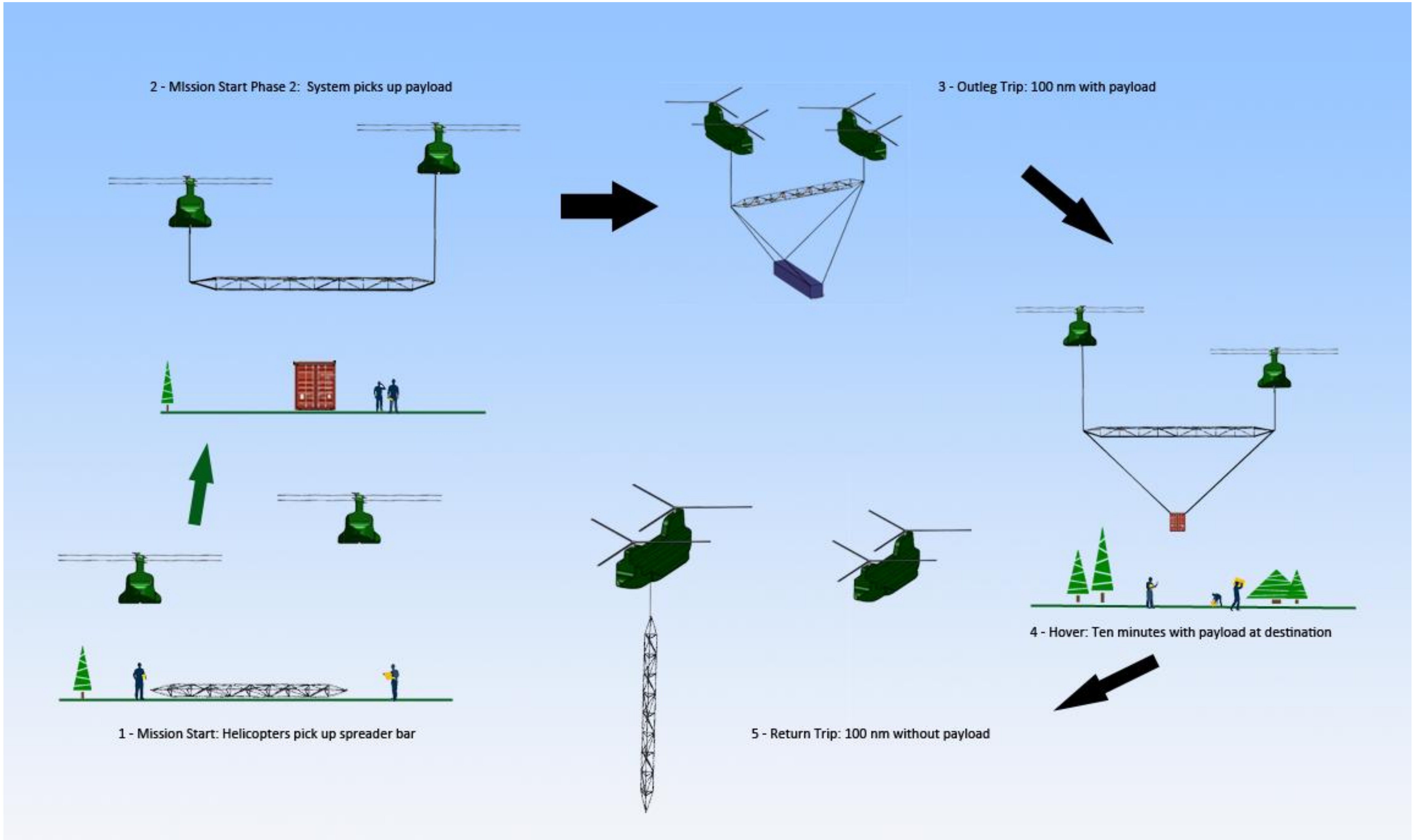

Figure 12-1: SPARCL Mission Diagram

Works Cited

"Aluminum Round Tube." *MetalsDepot*. Ledford Steel Company, 1999-2010. Web. 24 May 2010. <http://www.metalsdepot.com/products/alum2.phtml?page=rndtube&LimAcc=%20&aident=>.

Battlefield Recovery and Evacuation of Aircraft. Washington DC: , 2000. Web. 12 April 2010.

Curtiss, H.C. and Warburton F.W. "Stability and Control of the Twin Lift Helicopter System," *Journal of the American Helicopter Society*, April 1985, Vol. 30, pp.14-23

"Extruded Aluminum Tube 6061 T6 ." *OnlineMetals.com*. ThyssenKrupp Materials, NA, 1999-2010. Web. 26 May 2010. <http://www.onlinemetals.com/merchant.cfm?pid=9569&step=4&showunits=inches&id=71&top_cat=60>.

Gordon IV, John, Peter A. Wilson, Jon Grossman, Dan Deamon, Edwards, Mark, Lenhardt, Darryl, Norton, Dan, and William Sollfrey. *Assessment of Navy Heavy-Lift Aircraft Options*. Santa Monica, CA: RAND Corporation, 2005. xii. Print.

Hess , R.A. and Tran, P.M. "Pilot/Vehicle Analysis of a Twin-Lift Helicopter Configuration in Hover," *Journal of Guidance, Control, and Dynamics*, Vol. 11, No.5, Sept. 1988.

Hibbeler, R.C. *Engineering Mechanics: Statics*. 10th. Upper Saddle River, New Jersey: Pearson Prentice Hall, 2004. 260-67. Print.

Hibbeler, R.C. *Mechanics of Materials*. 6th. Upper Saddle River, New Jersey: Pearson Prentice Hall, 2005. 673, "Average Mechanical Properties of Typical Engineering Materials (U.S. Customary Units)". Print.

Hoerner, Sighard F. *Fluid Dynamic Drag*. Hoerner Fluid Dynamics, 1965. Print. United States.

Juska, Dr. Thomas. "Fibers (PowerPoint)." AERSP 473 (Class). Department of Aerospace Engineering. The Pennsylvania State University, University Park, Pennsylvania. 20 Jan 2010. Lecture.

Lexocable. "Wire Rope - LexcoCable.com." *Wire Rope, Aircraft Cable, Cable Assemblies | Lexco Cable*. Web. Mar.-Apr. 2010. <http://www.lexcocable.com/wire-rope.html>.

"Lifting Gears for Containers, General and Heavy Cargo." *Container Technics*. N.p., 02 Feb 2010. Web. 12 April 2010. <http://www.containertechnics.com/>.

Meirovitch, Leonard. *Elements of Vibration Analysis*. New York: McGraw-Hill, 1986. Print.

Multiservice Helicopter Sling Load: Basic Operations and Equipment. Washington, DC: Headquarters, Dept. of the Army, U.S. Marine Corps, Dept. of the Navy, Dept. of the Air Force, U.S. Coast Guard, 2006. Print.

Operators Manual for Army CH-47D Helicopter. Department of the Army, 2001. Print.

Reynolds, H.K. and Rodriguez, A.A. " Control of a Twin Lift Helicopter System," Proceedings of the 31st Conference on Decision and Control, Dec. 1992.

"Twin-Path Slings by Safety Sling." *Wire Rope, Wire Rope Slings, Chain Slings, Nylon Web Slings by Safety Sling*. Web. 20 Mar. 2010. <http://www.safetysling.com/tps.htm>.

Weber, J.M., T.Y. Liu, and W Chung. United States. *A mathematical simulation model of the CH-47B helicopter*. , 1984. Print.